European Commission

JRC SCIENTIFIC INFORMATION SYSTEMS AND DATABASES

Applications and results for the E-Nexus decision support system for the WEFE Senegal project

Climate Variability

Cattaneo L., Pastori M., Cordano E., Crestaz E., Seliger R., Koundouno J., Bausa Lopez L., Carmona C.

Sensitive

2019

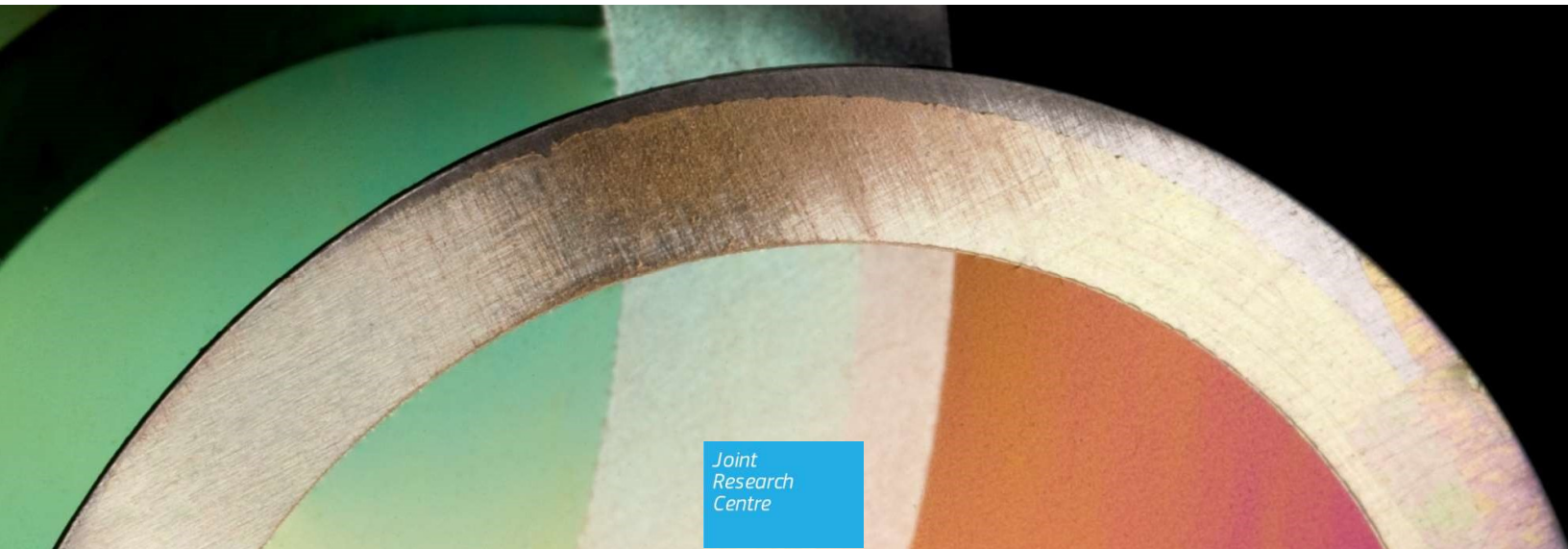

This publication is a Scientific Information Systems and Databases report by the Joint Research Centre (JRC), the European Commission's science and knowledge service. It aims to provide evidence-based scientific support to the European policymaking process. The scientific output expressed does not imply a policy position of the European Commission. Neither the European Commission nor any person acting on behalf of the Commission is responsible for the use that might be made of this publication.

Contact information
Name: César Carmona-Moreno
Address: Joint Research Centre, Via Enrico Fermi 2749, TP 440, 21027 Ispra (VA), Italy
Email: cesar.carmona-moreno@ec.europa.eu
Tel.: +39 0332 78 9654

EU Science Hub
https://ec.europa.eu/jrc

JRC115134

Ispra: European Commission, 2019

How to cite this report: Cattaneo L., Pastori M., Cordano E., Crestaz E., Seliger R., Koundouno J., Bausa Lopez L., Carmona, C.., *Title Applications and results for the E-Nexus decision support system for the WEFE Senegal project*, European Commission, Ispra, 2019, JRC119391.

Printed in Italy

Contents

Acknowledgements

This work is a part of the WEFE-Sénégal project funded by the European Commission.

Authors

European Commission, Joint Research Centre (JRC), Ispra, Italy

Abstract

This report is aimed to give an overall description of the features provided by E-Nexus tool and to display and analyse the results achieved so far within the frame of WEFE (Water Energy Food Ecosystems) Senegal project. It was initially developed in 2017 in order to support the local stakeholders in the Mékrou River Basin area, involving the countries of Niger, Benin, Burkina Faso (Udias et al., 2018). Then, it has undergone several updates and structural revisions with the oncoming project related with Senegal Basin area, to have it fit properly the necessities of the local features to be analysed and estimated via modelling and predictions tools. At the current moment, most efforts have been spent to produce an adequate study of the area, so, other than modelling and climate variability indices previously developed, it has been improved with evaluation tools for the analysis of seasonal dry spells (quantiles, trends, etc.) and global surface water variability. In this way, it can serve as a reliable Decision Support System for Environmental Monitoring through the detection of environmental trends and anomalies at the river basin level.
Giving a focused scope on the basin area, this report briefly describes the featured processes used by E-Nexus for every analysis performed on the basin, and then it displays the produced results along with an explanation of every detected behaviours in term of climate variability.

1 The WEFE Senegal Project

Figure 1: Senegal River Basin area, marked in black

The Senegal river is formed by the flowing of Bafing and Bakoye in Bafoulabé (Mali), and furtherly merged with Kolimbiné and Falémé, measuring a total length of 1800 km and a basin surface of 300 000 km^2. It is the second longest river in Western Africa, after the Niger river: the main tributary is the Bafing, with a length of about 800 km and whose sources are born from the Fouta Djalon Massif; The Falémé join the main Senegal river about 50 km upstream of Bakel. The other tributaries, much less important for water contributions are the Kolimbiné and the Karakoro. The Senegal river basin is charaterised by a tropical humid condition in the souther part, but the rest of the basin has a sub-Saharan dry climate. The basin is commonly subdivided into three zones: the upper basin (haut bassin), which is mountainous in Guinea, the Valley and the delta, which is a source of biological diversity and wetlands. Climatic, hydrological, landuse and topographical conditions are much different in these three regions and also season temperature and precipitation variations are extensive. In the Upper basin precipitaton are normally high (> 1800 mm/year), the slopes are severe and substrate is low permeable. The valley is indeed charaterized by low slopes and low precipitation input. In terms of water management and impact on food, agricultural systems and energy sectors the Manantali dam is one of the most important in the region: it is on the Bafing River, with an estimated volume of about 3.4 billion of m^3 covering a surface of 275 km^2 and the installed capacity of 200 MW. Another important dam in the region of Delta is the Diama dam, providing an important downstream water reserve capacity (for irrigation and civil water demands) and to prevent salty water intrusion from the sea.

As visible on the map (Figure 1), the total area is a result of a transboundary basin shared among the following countries: Senegal in the north-west with a percentage of 22%, Mauritania in the north (30%), Guinea in in the south (10%) and Mali in the middle-east (38%). In such large and complex background, elements like Water, Energy, Food and Ecosystems (WEFE) are inextricably linked to population well-being, poverty reduction and sustainable development, and all together are strongly bound to the environment.

In the Senegal River basin, there are various issues of environmental degradation, themselves exacerbated by the effects of climate change, as well as a strong interdependence between water supply security, food security and energy security (NEXUS). This interdependence must, in particular, be taken into account in the management of the Manantali and Diama dams (multiple-use dams), and the future Gourbassi and Koukoutamba dams among others. In the middle valley and delta, agriculture is the main activity that employs a large part of the working population and provides most of the household income. Better knowledge and control of the natural resources of the basin shall enable the decision-makers to promote an adapted river regulation process for, among other things, electricity production, irrigation development, traditional flood recession crops development and water supply for national parks (the Djoudj bird park in Senegal and the Diawling in Mauritania) and cities (in particular Dakar and Nouakchott).

The climate change effect (CC) has already started to alter the agricultural production by leading to an increased frequency and intensity of extreme events such as droughts and flooding at global scale (Cohn et al., 2017; FAO, 2016; Lesk et al., 2016; Lipper et al., 2014), with a particular negative impact on the coltures of Western African Sahel (Zougmoré et al., 2016), despite it has been brougth to evidence that most of the productivity loss of this region is normally caused by a poor soil fertility management (Van Keulen and Breman, 1990). Under such circumstances, it is imperative to mark the key factors which may play a major role for any improvement strategies in the field of agriculture and a general optimisation of the environment resources in order to to better achieve sustainable outcomes.

The execution of a trend analysis of all climate behaviours interesting the area, using models to evaluate future scenarios and possible risks induced by climate change, is an useful way to assist the OMVS (*Organisation pour la mise en valeur du fleuve Sénégal*), the regional organisation mandated by the four member States for managing the river basin sustainably, into its strategies concerning the development of the area. It is also useful to estimate any vulnerability of the river dams and plan proper managing policies for an overall improvement of the hydrologic resources. In addition, it takes to evaluate the current kwnoledge of basin populations about climate issues and consequent impacts, and hence provide adequate information services to the locals to contribute on achieving a correct perception of such phenomena and help them to adaptation and face induced extreme events, to contain - and possibly avoid - any socio-environmental crysis brought by such anomalies.

For the last decades, the WEFE Nexus approach has been providing a comprehensive image by gathering all described elements (water, energy, food), in order to display all connections among all of them and describe the way they affect each other and how they rely on and impact ecosystems. Therefore, it is always worth to improve this strategy and achieve better life conditions of the local population.

With such premises, the major concerns expressed by local stakeholders and organisations can be enumerated as follows:

- Population growth and change of life quality standards and food demand;
- Urbanization issues
- Energy demand increase
- Raising competition for water demand by different sectors
- Climate change and specific impact on water availability on spatial and temporal scale
- Environmental degradation

Bio-physical models associated to relevant socioeconomic analysis within robust Decision Support Systems (DSSs), if properly designed, can provide a unique assistance to OMVS and their partners into a wide range of fields for water, energy and food security : agricultural production and livestock management, land management systems, environmental planning, multipurpose dam optimization etc.

2 Introduction of the system

Since the first stages of its development, it has been clear that the E-Nexus tool was expected to serve for a multiple range of purposes involving environmental analysis and modelling, given the number and nature of tools it was going to implement and perform as internal routines. As Figure 2 shows, its multi-module based structure has made it able to progressively host an increasing number of evaluation tools and standalone models. More specifically, it is able to operate at different scales and carry out climate variability analysis out of climate series, execute EPIC and SWAT simulations in order to produce predictions over hydrology and agriculture data, and run optimization algorithms for water and crop management.

With this premises, the module results to play a key role in decision making processes aimed at the evaluation of suitable solutions and policies for improving management of local resources through comparing the trade-offs of every produced scenario, each one based on distinct optimization strategy. As a goal of WEFE Senegal, the E-Nexus is intended to assist as Decision Support System (DSS) in order to enhance the performance of existing technical structures and analysis interfaces already operating in the area, and thus contribute to build a better overall assessment service of all project components (Cattaneo et al., 2018).

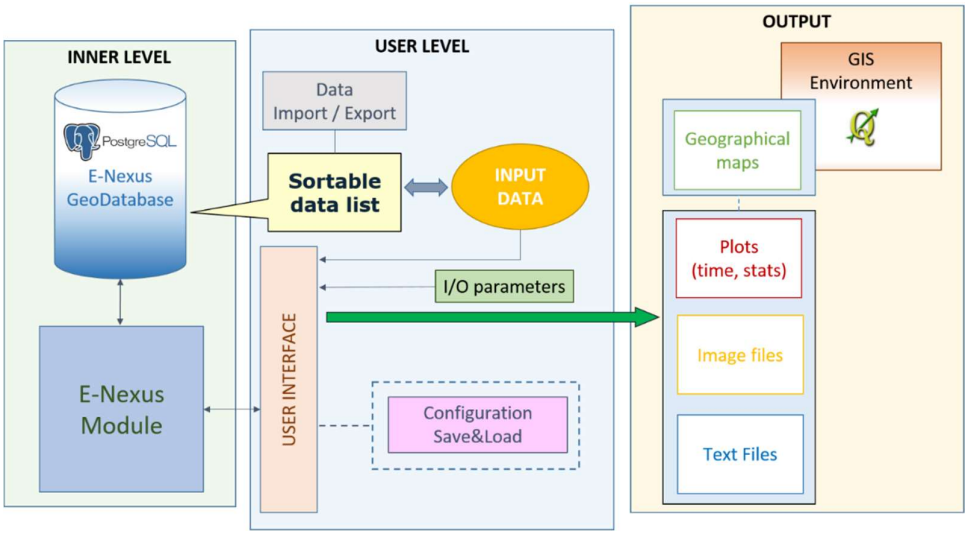

Figure 2: Schematic representation of the E-Nexus open source framework.

More in detail, it is expected to achieve the following results:

- Attuning and updating existent routines in order to have them compliant to the requirements of Senegal River Basin region (this includes checking for new input datasets and a partial recalibration of EPIC and SWAT models)
- Extending the climate variability tools by providing new indices, such as indices related to dry spell analysis (length, trend, etc.)
- Enhancing optimization algorithm by adding direct connections with other internal tools provided by E-Nexus (e.g. models and predictions), and providing other key factors involving livestock management and analysis of economic fluctuations (crop market) for better overall results
- Developing a dedicated section concerning renewable energy strategies (e.g. Biogas and PV)
- Improving the socio-economics section to produce deeper and more accurate simulations about livelihoods, human well-being and inclusive development policies

The most direct way leading to a successful assessment of water resources over the whole year is to perform a climate variability analysis: through the evaluation of return periods and critical values from temperature and precipitation time series, it is possible to plot trends and fluctuations concerning the climate behaviour of interested areas (from regional to global scale). Such evaluations are able to provide an interesting contribute for the evaluation of future land use strategies and even to estimate the risk of possible extreme events, which may pose a serious threat to local population and environment resources. For these reasons, retrieving an adequate variety of input datasets covering the longest possible period over the basin area was among the first goals related to the adaptation procedures to be carried out on the E-Nexus.

Regarding the processes involving hydrologic and agriculture models, it has to be pointed that the most consistent predictions can be necessarily be achieved by improving input datasets with a proper set of observations provided by local stations. So, this last year has been dedicated to perform all setup processes involving data validation and model calibration for a reliable performance of the analysis tools.

Given the necessity of addressing it to the widest possible range of users, E-Nexus is a stand-alone desktop application conceived for Windows OS mainly built using .NET languages (C#, Basic), but it also incorporates R libraries and scripts for internal processes involving statistics and algorithms. Since this module exclusively relies on open-source software, it is possible to use it without purchasing any particular license apart from Windows system.

3 E-Nexus Climate variability indices explanation and results for the Senegal river basin

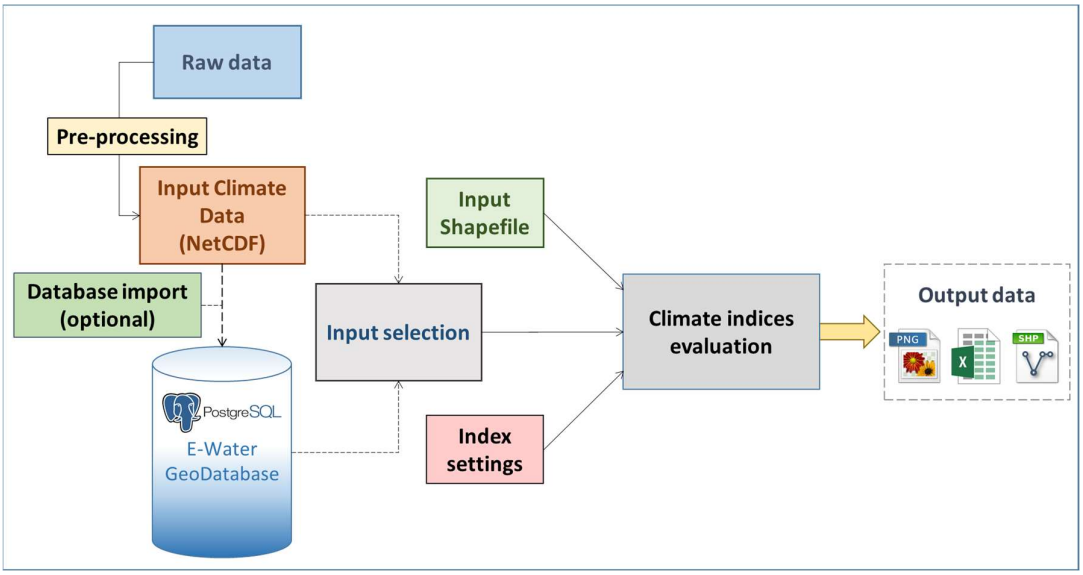

Figure 3: Process diagram of E-Nexus Climate menu.

Climate variability processes are provided by E-Nexus through Climate interface. All processes in this section are aimed to give products on a space – time scale (usually maps and plots) in order to describe the occurrence of extreme events related to temperature and precipitation by using statistics algorithms based on L-moments evaluation.

Possessing a detailed knowledge of climate variability and climate change trends at different scales (from local to continental) is simply crucial for everyone who is involved in the socio-economic development policies relative to the basin domain - either researchers, policy makers or stakeholders. In fact, anomalies and extreme events may have strong consequences on crop yields, hydrologic resources and livelihoods, so dealing with them in advance is key to prevent food and water shortage, reduce the risk of famine and poverty.

Figure 3 describes the general structure of climate processes: after pre-processing raw data (usually aggregating a set of multiple files into a single one), input data can be provided through either local files (NetCDF) or PostgreSQL tables, whereas outputs are internally saved as images with equivalent vector files (TIFF format, easily manageable through GIS interfaces) and documents .

As Table 1 shows, from this section it is possible to evaluate the following indices: return periods and related values (both temperature and precipitation), heat waves (temperature), dry spells, excess/deficits and SPI (precipitation). To assess the occurrence probability and the return periods related to extreme events like droughts and heat waves, the module applies a L-Moments methodology on inputs of circa 35-year time series using the R package *lmom* (Hosking, 2017), available on the online CRAN repository.

For monthly data, it is either possible to process all the twelve months of the year, or select a limited list in order to focus the process on a particular period or season of the year (see interface on Figure 4).

Variable	Aggregation	Index
Precipitation	Daily	Dry spells
	Monthly Maximum (mm/day)	Return periods (monthly/annual/custom)
	Monthly Sum (mm/mon)	Excess/deficit (monthly/annual) SPI Return periods (custom)
	Annual Maximum (mm/day)	Return periods (annual)
Temperature	Daily	Heat waves
	Monthly Maximum	Return periods (monthly/annual/custom)
	Annual Maximum	Return periods (annual)

Table 1: correspondence between input aggregations and available climate variability indices.

In order to obtain all climate variability outcomes, the E-Nexus tool has utilized historical time series from the following temperature and precipitation datasets: ERA5 and MSWEP.

- **ERA5** is a new global climate reanalysis developed from ECMWF in 2016 through the Copernicus Climate Change Service (C3S), providing historical datasets from 1979 to the present (Hersbach et al., 2018). It has developed as an update of its previous version the ERA Interim dataset, which provided hydro-meteorological variables across land at multiple temporal scales (up to 3 hours). It is based on 4D-Var data assimilation routines, performing Cycle 41r2 of model IFS (Integrated Forecasting System). In order to reduce the ensemble spread and produce the most reliable forecasts possible, it also features a 10-members uncertainties detection system at sub-daily scale (3 hours) spanning at 63 km-resolution. Compared to its predecessor, it features an improved horizontal resolution (from 79 to 31km-squared cell), more pressure levels (from 60 to 137, with an interval of 1 Pa), other than an extended list of output parameters. Starting from 2020, it is expected to have an improved base of data, featuring historical series from 1950 onwards. ER5 data is available in GRIB and NetCDF formats.

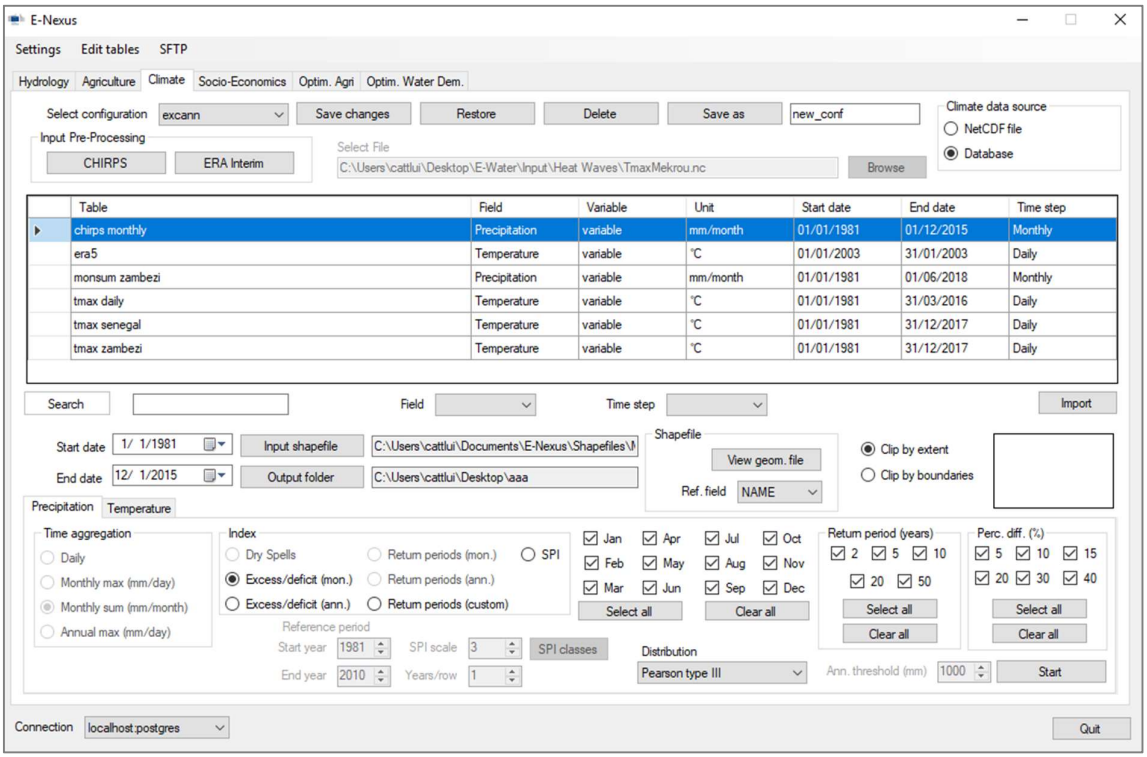

Figure 4: Graphical interface of E-Nexus Climate menu

- The Multi-Source Weighted-Ensemble Precipitation (**MSWEP**) is a precipitation dataset providing 3-hour rainfall estimations on a high resolution grid of 0.1° on a world scale. Being updated to the second version (V2) in 2019, it is able to produce data from 1979 to 2019 obtained by merging output values from gauges (WorldClim, GSOD, CHCN-D, etc.), satellites (GridSat, GSMap, TRMM, etc.) and re-analyses (ERA-Interim, JRA-55), and correct them with daily observation gathered from over 70000 gauges(Beck et al., 2017; Beck et al., 2019). As a result, precipitation values have revealed a high correlation when compared directly with station outputs. Hence, MSWEP is a valid tool to assist hydrologic modeling and perform studies involving precipitation variability on heterogeneous environments.

3.1 Precipitation deficit

The evaluation process of precipitation variability is based on a close dependence between the deviation rate of monthly cumulates over their average, both positive (excess) and negative (deficit), and the return periods corresponding to such variations. In this specific case, the general process has been performed for each 0.1°-sided grid cell of rainfall historical series from MSWEP dataset, focusing on the months between June and October, characterized by the most relevant precipitations, of period 1981-2016. Among the outputs of interest, variability analysis has produced a set deficit maps for the whole area, each one related to given return period (from 5 to 50 years). As Figure 7 and Figure 8 show, deficit represents the percentage variation from average monthly precipitation with an occurrence defined by return period (values with RP5 are expected to be reached once in five years, and so on): displayed results may vary from 0% (precipitation corresponding to its exact average) to 100% (no rainfall).

Monthly precipitation mean (1981-2016)	Monthly precipitation variability (L-CV) (1981-2016)
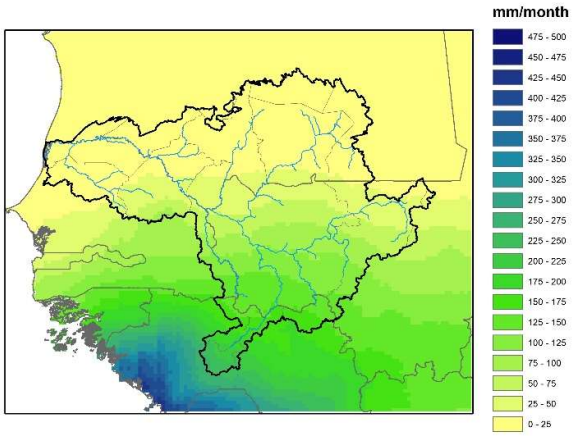	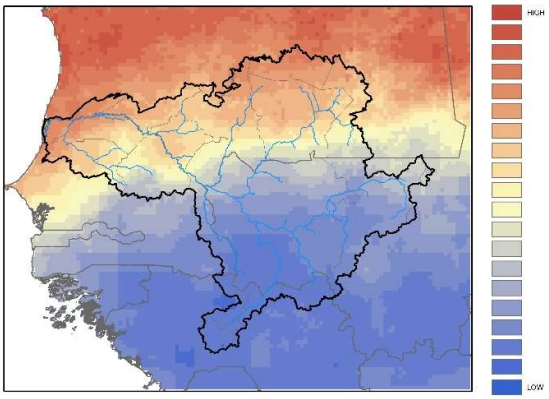
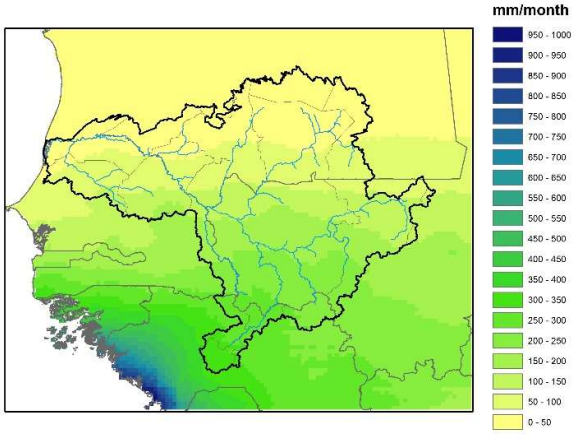	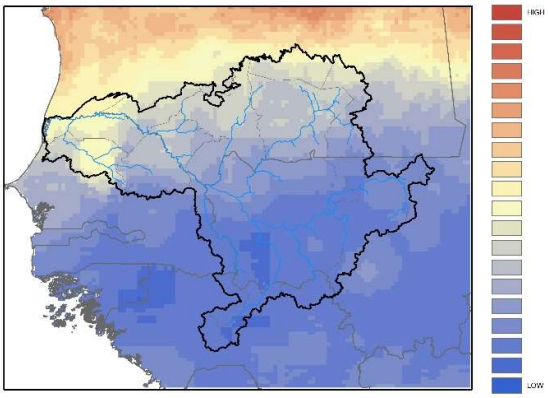
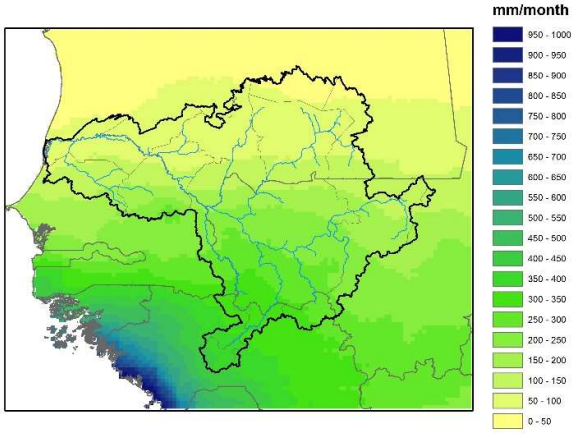	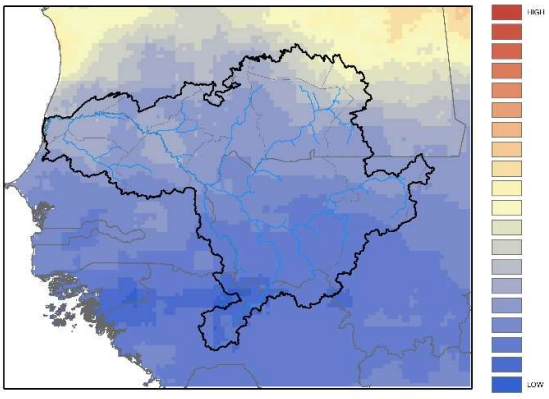

Figure 5: monthly precipitation mean (left) and L-CV variability (right) for the months of June (1st row), July (2nd row) and August (3rd row) over Senegal River Basin from 1981 to 2016

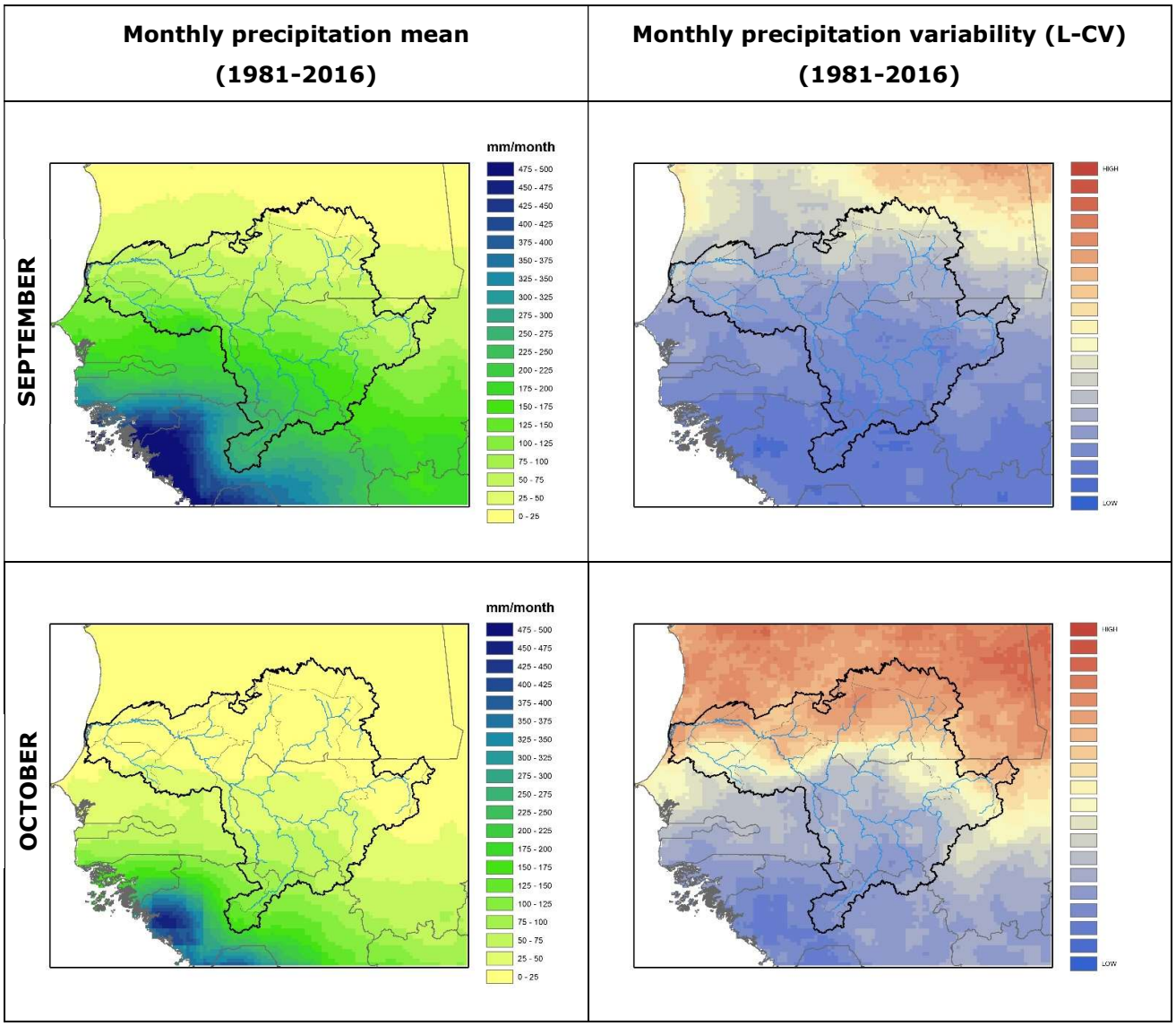

Figure 6: monthly precipitation mean (left) and L-CV variability (right) for the months of September (1st row) and October (2nd row) over Senegal River Basin from 1981 to 2016

The input data has been modelled using the Pearson-III distribution: being more flexible and allowing a better fit to any number of rainfall regimes with reasonable accuracy, such statistical method is considered as a good choice for describing cumulated precipitation values. Mean and L-CV variability (average-normalised standard variation), obtained through L-Moments evaluation, are also useful to illustrate the base values which are therefore affected by any potential deficit, and may help to return the effective relevancy of detected oscillations (see Figure 5 and Figure 6).

Normally, before checking for deficits in a particular area, it is useful to verify if it also registers a relevant amount of precipitation with significant average values. Otherwise, even limited variations could induce a high deficit rate: the northern part of the map is a desert region and shows this behaviour, so it is of no interest for the variability studies above described.

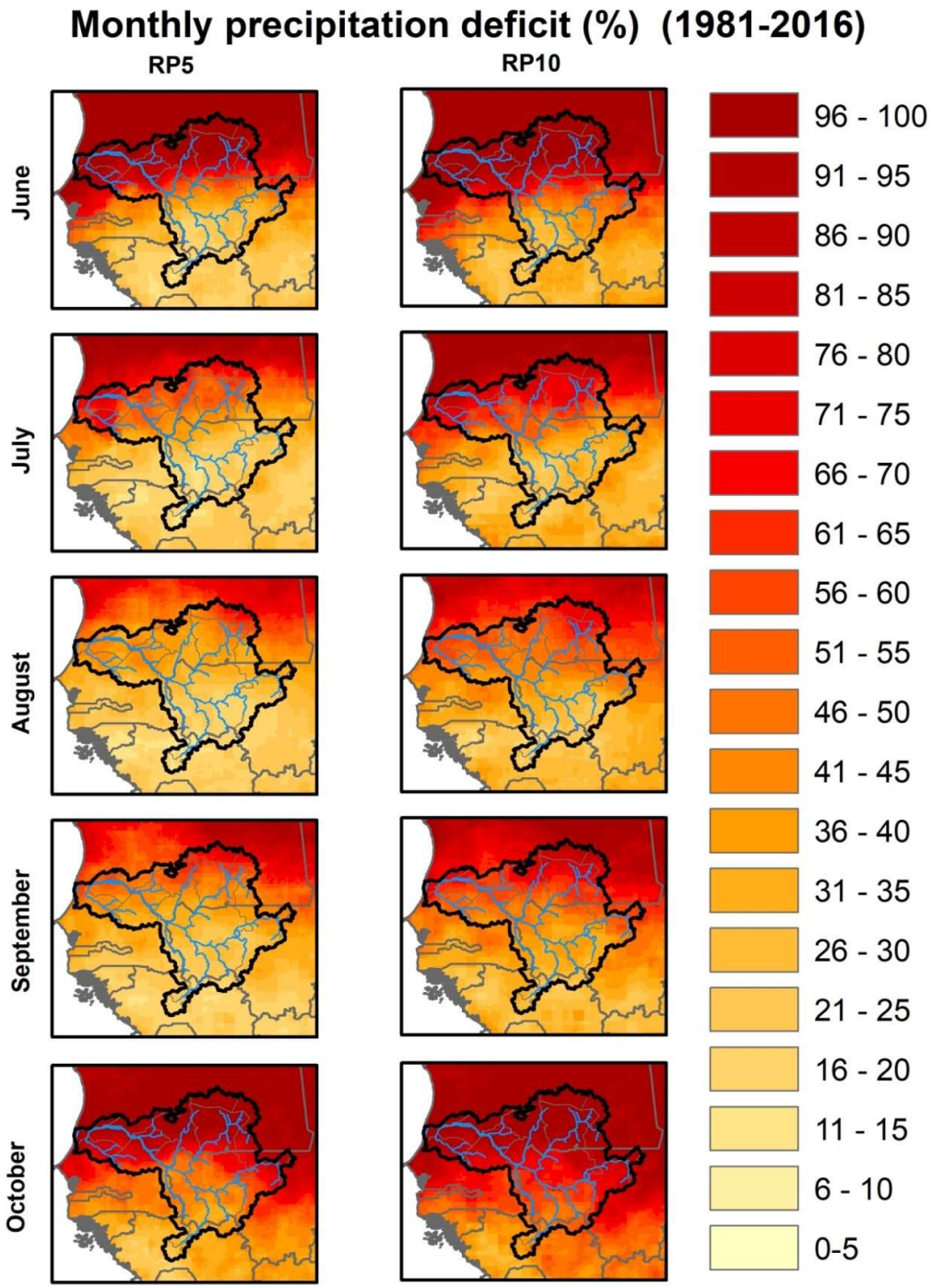

Figure 7: monthly precipitation percentage deficit related to return periods of 5 years (left column) and 10 years (right column) for the months from June (1st row) to October (5th row) over Senegal River Basin for period 1981-2016

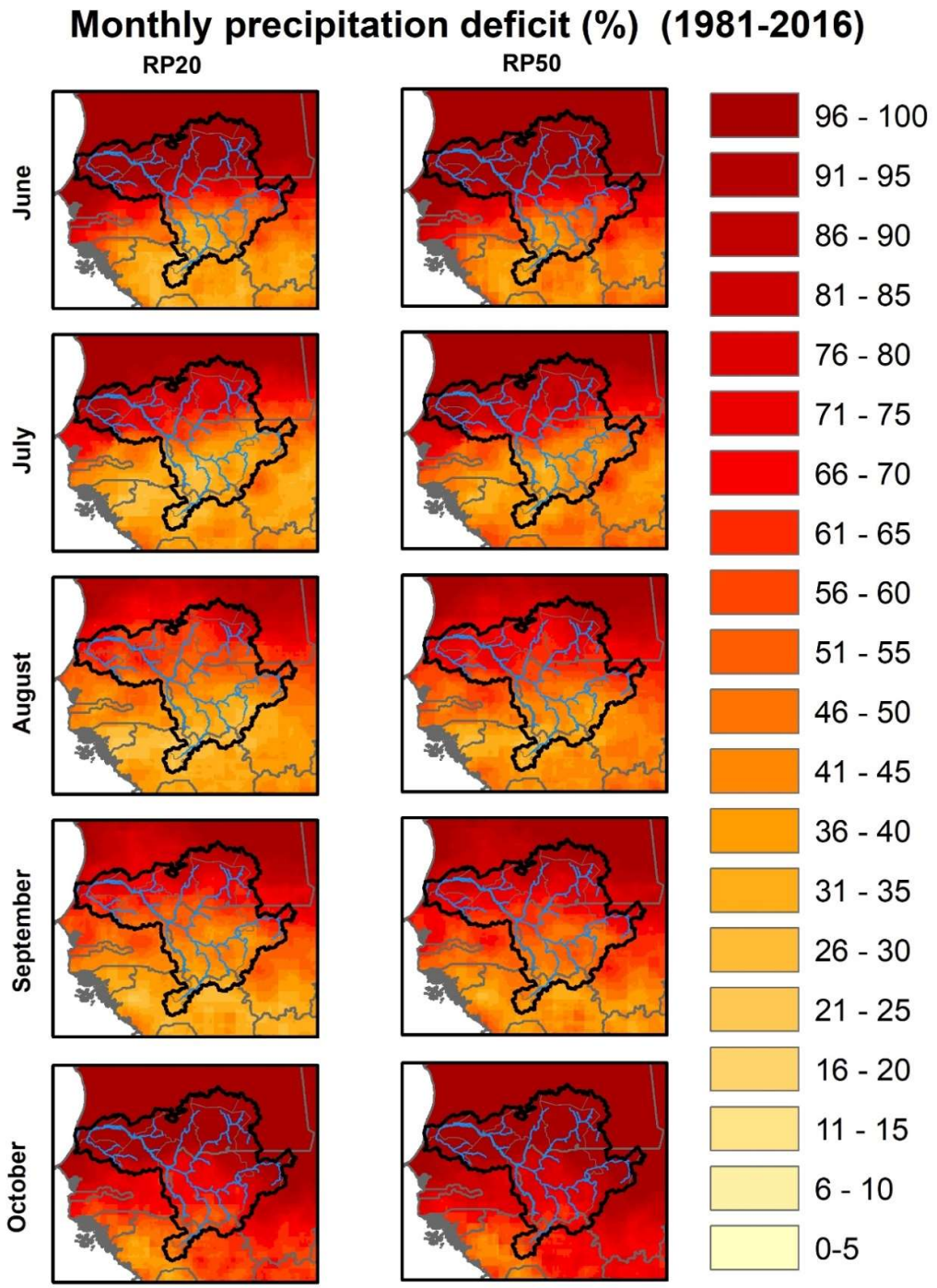

Figure 8: monthly precipitation percentage deficit related to return periods of 20 years (left column) and 50 years (right column) for the months from June (1st row) to October (5th row) over Senegal River Basin for period 1981-2016

From the monthly means, it is evident that southern latitudes show generally a higher precipitation rate, and the most relevant rain percentage is measured in the months of July and August with peaks of over 400 mm/month in the Fouta Djalon area (south). After giving a look at the deficit maps, it is easy to notice that deficit tends to decrease in areas hit by significant precipitations, usually showing a rainfall reduction spanning from 15% every 5 years (RP5) to 50% once in 50 years (RP50). The overall image is that rains are fairly regular in most of the basin area, with the most significant droughts occurring only with high return periods and affecting the driest months of this period. Under this perspective, the outcomes of October have the rainfall values with the highest deficit susceptibility (up to 70%), when compared to other months with similar precipitation rates.

3.2 Heat Waves

The *Heat Wave Magnitude Index daily* (HWMId) has been recently defined as a simple numerical indicator that takes both the duration and the intensity of the heat wave into account (Russo et al., 2015), and it has also been applied for climate studies in the African context (Ceccherini et al., 2017). Evaluated as the maximum magnitude of the heat waves in a year, the HWMId is an improvement on the previous Heat Wave Magnitude Index (HWMI, Russo et al., 2014) and it is able to overcome its limitations. More precisely, HWMI suffers from a limited value range and has some problems in assigning magnitude to very high temperatures in a changing climate, thus resulting in an underestimation of extreme events.

Classification	**Heat Wave Magnitude Index daily**
Normal	$1 \leq HWMId < 3$
Moderate	$3 \leq HWMId < 6$
Severe	$6 \leq HWMId < 9$
Extreme	$9 \leq HWMId < 15$
Very extreme	$15 \leq HWMId < 24$
Super extreme	$24 \leq HWMId < 32$
Ultra extreme	$HWMId \geq 32$

Table 2: Classification of heat waves (i.e. HWMId) scale categories

More in detail, a heat wave is a period of three or more consecutive days with maximum temperature above a daily threshold corresponding to 90th percentile over a reference period of 30 years. The evaluation of maximum temperature percentile is narrowed on a 31-day window centred on that particular day, which is repeated for every year of reference period: in this way, there will be a percentile available for each day of the year (tot. 365). The inter quartile range (IQR, namely the difference between the 25th and 75th percentiles) of the daily maximum temperatures is used as the heat wave magnitude unit, since it represents a non-parametric measure of the variability. Then, if a day of a heat wave has a temperature value equal to the 75^{th} percentile, its corresponding magnitude

value will be equal to one. According to this definition, if the magnitude value on a given day is 3, it roughly corresponds to an anomaly of 3 times the IQR. Finally, the total value of a heat wave magnitude is the sum of all daily ones.
The HWMId index could be classified with using a succession mainly composed by multiples of three, as shown on Table 2.

Figure 9 shows results about the incidence of heat waves in the Senegal River Basin collected from ERA5 maximum daily temperatures over the period 1979-2018, evaluated from the reference period 1979-2008. It is easy to notice that the most relevant heat waves have occurred in the period 1997-1999, showing HWMId values around 10 (labelled as *extreme*) in the central part of the basin, mostly shared by Senegal and Mali.

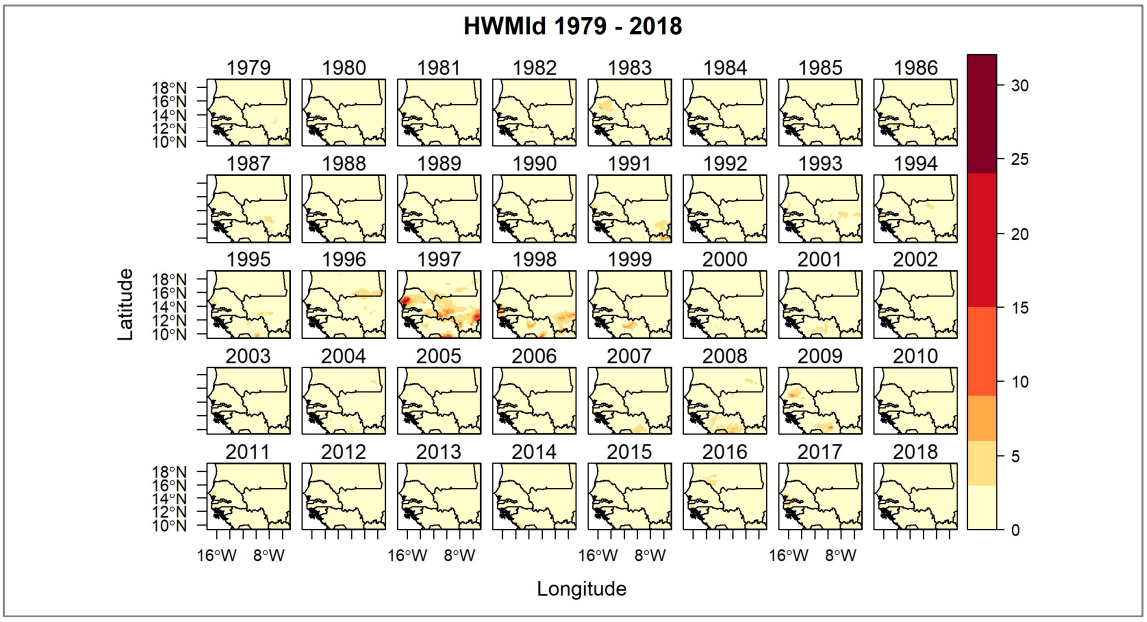

Figure 9: Yearly Heat Wave Magnitude Index between 1979 and 2018 in Senegal River Basin

Such outcomes are used to build the resume map on Figure 10, counting on each point the occurrence of HWMId exceeding the threshold value of 4, commonly associated to heat waves of noticeable intensity (3 consecutive days with maximum temperature significantly above the IQR). In this way, it can be noticed that the most intense anomalies are registered in the Senegal (west) and Guinea (south) regions.

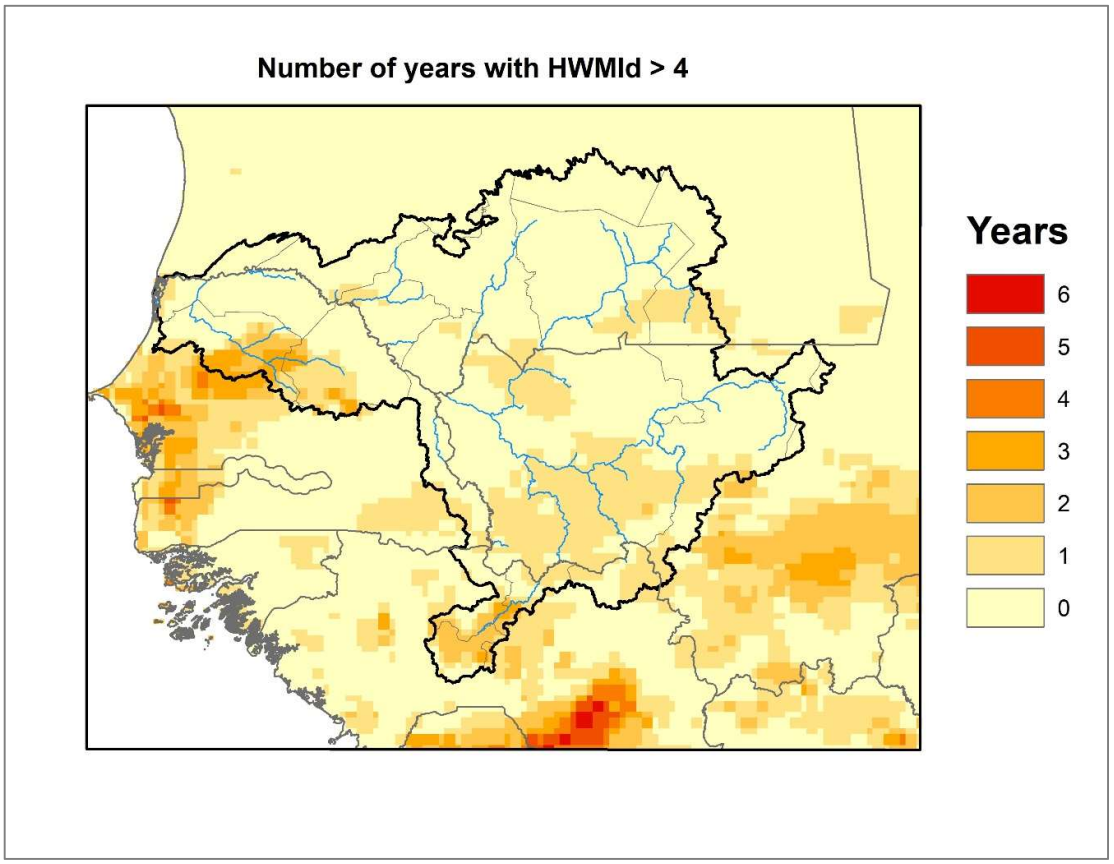

Figure 10: number of years within 1979 and 2018 with HWMId exceeding values of four

3.3 Standardized Precipitation Index

The Standardised Precipitation Index (SPI) allows the evaluation of precipitation anomalies and droughts affecting different geographical domains. It can be used along with other indices in order to estimate dry spells for hydrological and agricultural studies (Guttman, 1999). More specifically, SPI is a probability index based on monthly precipitations intended to provide information about extreme values of humidity and/or dryness with respect to the average behaviour. If normalised, it allows to evaluate a drought occurrence rate. SPI can be calculated for different temporal windows (generally, 1 to 36 months) taken from monthly input data: on short timescales, the SPI is closely related to issues interesting soil moisture, whereas longer timescales are used to analyse the effects on groundwater and reservoir storage. Commonly, the index is followed by a number indicating chosen monthly timescale (e.g. SPI-3 corresponds to 3 months, with March outcomes covering the period January - March).

SPI evaluation is carried out through the following three steps:

1. Using L-Moments, a probability density function (PDF) is set up according to the frequency distribution of monthly precipitations and the time scale of interest.
2. Reference period (30 years) is divided into 12 parts, each per month. Every data fraction, containing one monthly value per year, is then adjusted with a Pearson III statistical distribution.
3. Cumulated probability undergoes an inverse transformation of its standardised Gaussian distribution (centred on zero, unitary deviation), thus giving SPI a description in terms of difference from temporal average.

Since its time-space invariance, different SPI instances can be directly compared regardless of the climate zones they come from and their related annual period.

Wet/dry class	SPI values (Mckee et al., 1993)	SPI values (Agnew, 2000)
Extremely Dry	< -2	< -1.64
Severely Dry	[-2, -1.5]	[-1.64, -1.28]
Moderately Dry	[-1.5, -1]	[-1.28, -0.84]
Moderate	[-1, 1]	[-0.84, 0.84]
Moderately Wet	[1, 1.5]	[0.84, 1.28]
Severely Wet	[1.5, 2]	[1.28, 1.64]
Extremely Wet	> 2	> 1.64

Table 3: SPI-n classification

All the results of evaluated SPI-3 from 1981 to 2016, with the interval 1981-2010 chosen as reference period, are shown on Figure 11, giving an overall idea of the index trend within the year, other than its evolution throughout the whole period. The specific results on Figure 12 compare the outputs of August and September obtained in the years 1984 and 2012: while in the first year a general dryness is encountered in all the basin area with SPI values around -2, on the second year there is a totally opposite trend in with a wet behaviour in the central region. However, the entire series shows that the second half of the year (June to December) is more prone to be affected by dry anomalies, which can be explained by the fact that most of the precipitations concentrate on this period. Colour palette has been chosen using a classification with threshold values from Agnew scale, spanning from -1.64 (extremely dry) to 1.64 (extremely wet), as shown on Table 3.

The identification of moderately to extremely dry periods with respect to the average of registered rainfalls is particularly important when potentially near to the crop harvest period or during the main growing cycle as can potentially affects and reduce crop yield quantity and quality if not mitigated. Specific regional analysis can also be used: it is possible to estimate the SPI taking into account the surface of each administrative region that is affected by a specific anomaly. Produced results are therefore able to identify possible anomalies by spatial areas and distinct periods.

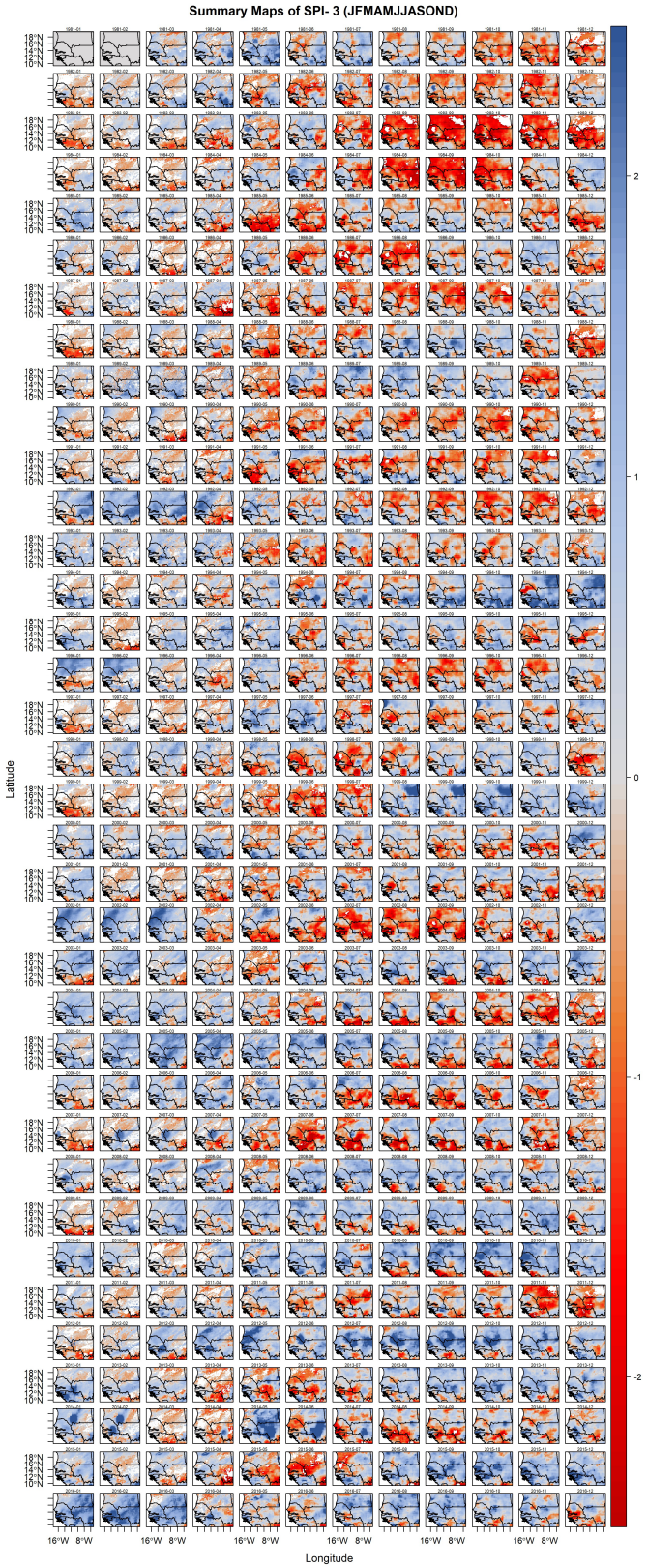

Figure 11: Summary Maps of SPI-3 for the whole period (1981-2016) over Senegal River Basin

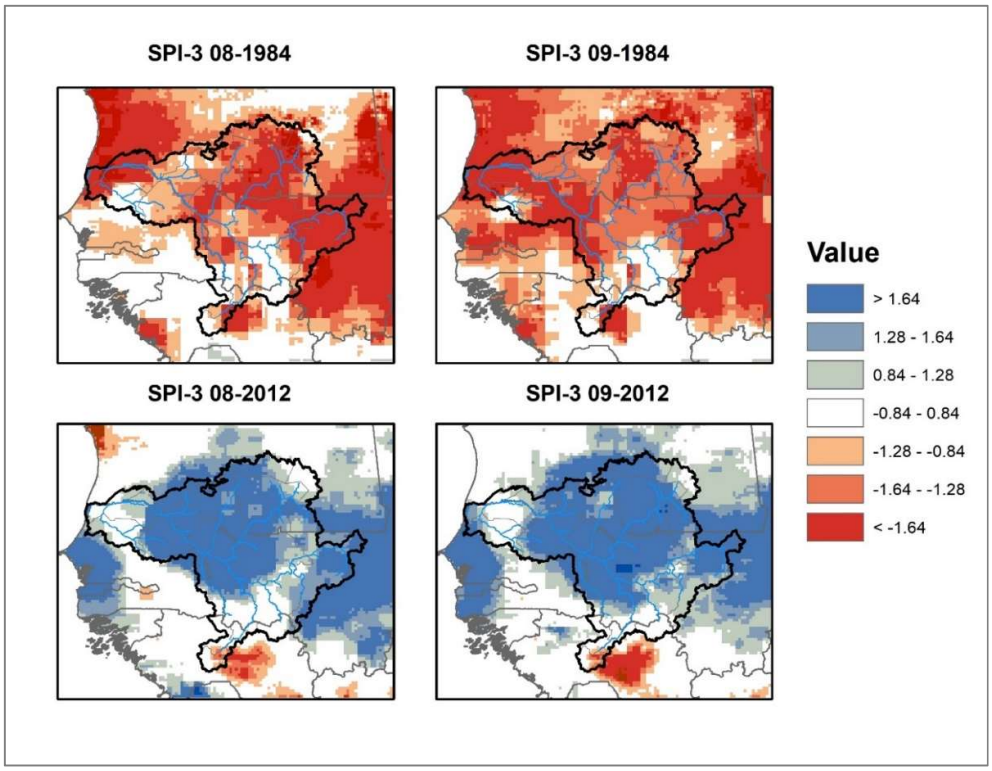

Figure 12: SPI-3 outcomes for the months of August (left) and September (right) of years 1984 (top) and 2012 (down) extracted from Figure 11

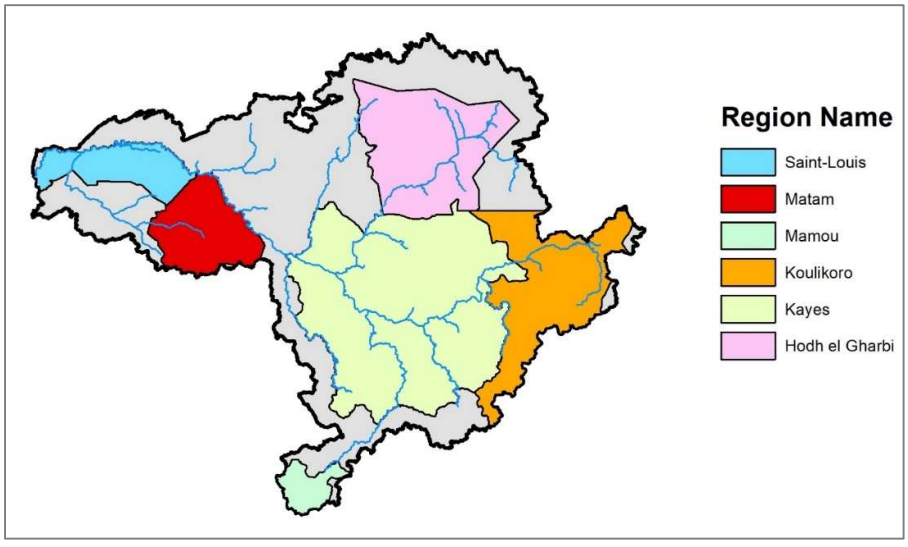

Figure 13: Selected administrative regions of Senegal River Basin for SPI analysis

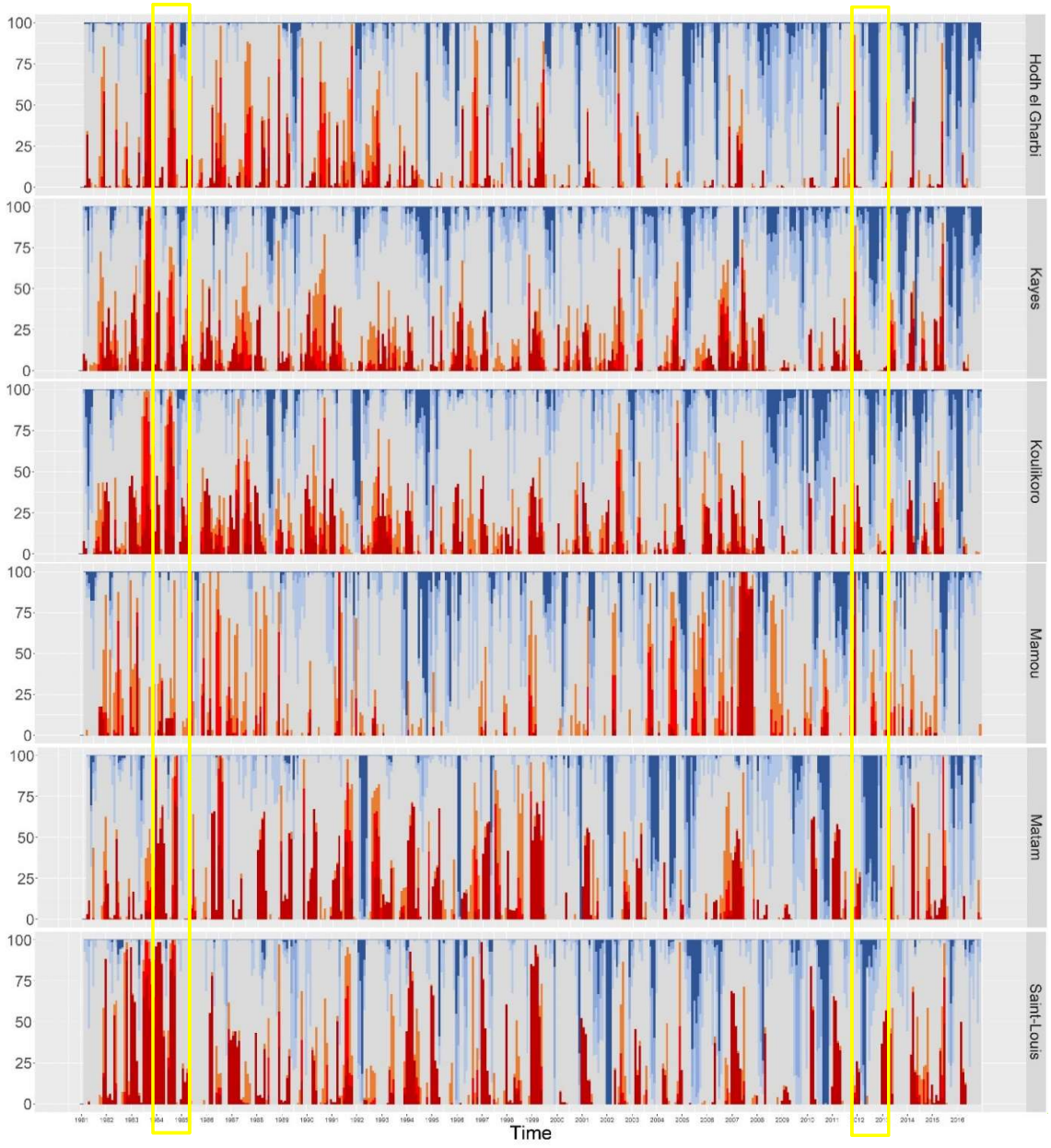

Figure 14: Surface distributions of SPI-3 for six regions of Senegal River Basin from 1981 to 2016. The yellow boxes point to sample values collected in 1984 and 2012.

To give a general idea of the surface distribution of SPI in specific administrative regions of Senegal Basin area, the following domains have been selected out of a total of 19:

- Saint-Louis (Senegal)
- Matam (Senegal)
- Mamou (Guinea)
- Koulikoro (Mali)
- Kayes (Mali)
- Hodh el Gharbi (Mauritania)

Further analyses are focused on such regions since the areas they cover within the basin (see Figure 13) are often interested by critical SPI values in the analysed period, as seen on previous outcomes.

For each region, the vertical lines represent the SPI-3 distribution over its surface, with colours varying from red (*Extremely Dry*) to blue (*Extremely Wet*) for every month in period 1981-2016, according to Agnew classification (Figure 14). When comparing these results with the SPI maps, it is possible to notice that the intense dryness registered in 1984 (see Figure 12) is clearly drawn into all domain plots as an intense red line. The central region of Kayes is considered an exception, since its large surface has a more sparse distribution of dry events, and Mamou, marginally less affected by this anomaly. When looking at the results of year 2012, which affected a great part of the basin area with intense rainfalls, such behaviour is consistently marked with wide blue lines in almost all regions (especially Matam, being entirely "covered" by high SPI values). In this case, a different behaviour is shown in the region of Mamou, which has been even interested by an opposite trend, with mild droughts located in some points of its surface. Other than described cases, a regular behaviour is represented as a periodic evolution within the single year, so the presence of unexpected values could probably correspond to anomalies brought by droughts or heavy rains (e.g. an intense dry event affecting Mamou region in 2007).

The analysis of SPI surface distributions may be helpful to evaluate the index evolution on temporal scale within particular zones interested by peculiar environment and climate condition, while spatial maps can be taken into account for a punctual analysis of the phenomena.

3.4 Dry spells

In the framework of Senegal project, climate variability analysis has also been conducted to the study of spatio-temporal dynamic patterns of dry spell periods during a particular season of the year, e.g. the growing season. Dry spells are defined as periods longer than a conventional threshold value of 3 consecutive days, characterised by a daily precipitation below 1 mm (Ratan et al., 2013; Chaudhary et al., 2017; Masupha et al., 2016; Froidurot et al., 2017).

Therefore, the detection of all dry spells from 1981 to 2016 is performed with suitable R functions (Cordano, 2015) for an area covering the entire Senegal River basin and its surroundings. The dynamics of this phenomenon are of great interest to detect the seeding periods at the beginning of the growing season, due to fact that crop growth is extremely sensitive to intermittence of dry and wet periods (Gornall et al., 2010).

In order to resume the overall variability behaviour during the latest decades, multiple aggregated indices have been evaluated for the growing season of each year: to calculate them, dry spells dynamics were extracted for the entire period of input precipitation time series.

After all dry spells are detected in the selected period of the year (generally, the growing season), the internal process perform a synthetic characterisation by aggregating them into single values to be easily displayed on spatial maps. In particular, output consists in a set of indices, each one extracted at annual frequency (for every year of the interval) and aggregated in general factors (mean, trends, etc.) referring to the whole period. The complete list of dry spell indices is displayed below on Table 4.

Index	Definition
drySpellCountLow	number of dry spells in selected period of low duration (3 to 10 days)
drySpellCountIntermediate	number of dry spells in selected period of average duration (11 to 21 days)
drySpellCountHigh	dr number of dry spells in selected period of average duration (more than 21 days)
drySpellCount	total number of dry spells in selected period
median	50th percentile of the duration of all dry spells in selected period
max	maximum duration of dry spells in selected period
q25, q75, q90	$25^{th}/75^{th}/90^{th}$ percentile of the duration of all dry spells in selected period
mean	average duration of all dry spells in selected period
q90_7	90th percentile of the duration of all dry spells longer than 7 days in selected period
iqr	difference between 75th and 25th percentiles (interquartile range - IQR) of all dry spells in selected period
sum	total duration of all dry spells in selected period

Table 4: list of dry spell indices provided by E-Nexus interface

The analysis of dry spell patterns has been preliminarily conducted for two different seasons: Northern Hemisphere Summer (JJA) and Autumn (SON), both composing the typical rainy season in Western Africa/Sahel Region. Precipitation values are taken from MSWEP Dataset and indices area evaluated from period 1981-2016. The following pages show the outcomes produced by the indices of *DrySpellCountLow*, *DrySpellCount*, *iqr*, *mean* and *q90*, offering an image of the general behaviour of dry spells in terms of quantity (number of occurrences) and intensity (spell length). Each index is represented through its average value and trend slope over the whole period, in order to give the most exhaustive idea about its evolution throughout the analysed years. The trends are obtained by Mall-Kendall statistical testing and significance assumption related to a p-value of 0.1, showing the values of their overall slope indicating whether the number or intensity of dry spells may averagely increase or decrease after every year.

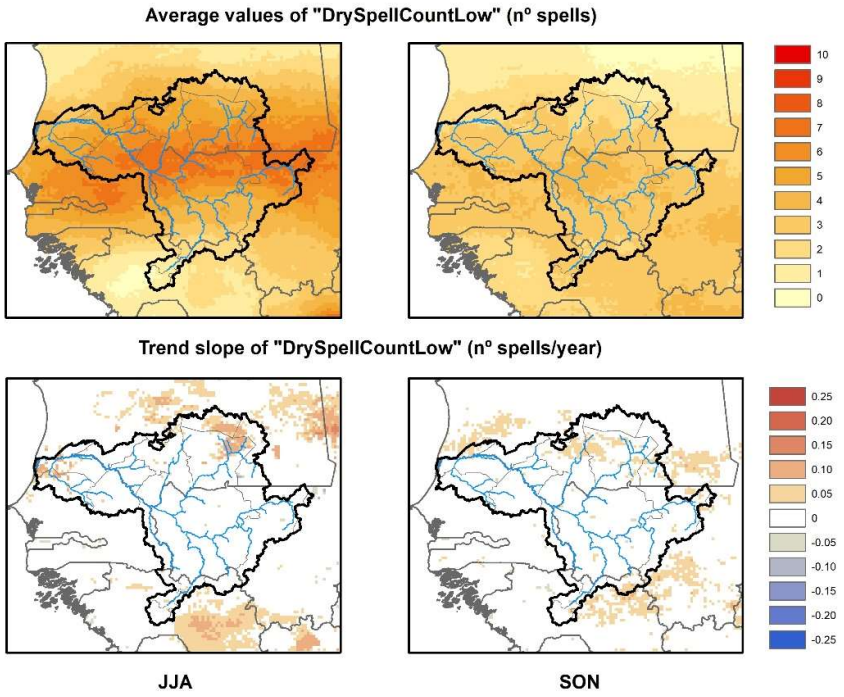

Figure 15: number of low duration dry spells (from 3 to 10 days) over Senegal River Basin from 1981 to 2016. Results are in form of average values (top) and trend slopes (down) for seasons JJA (left) and SON (right)

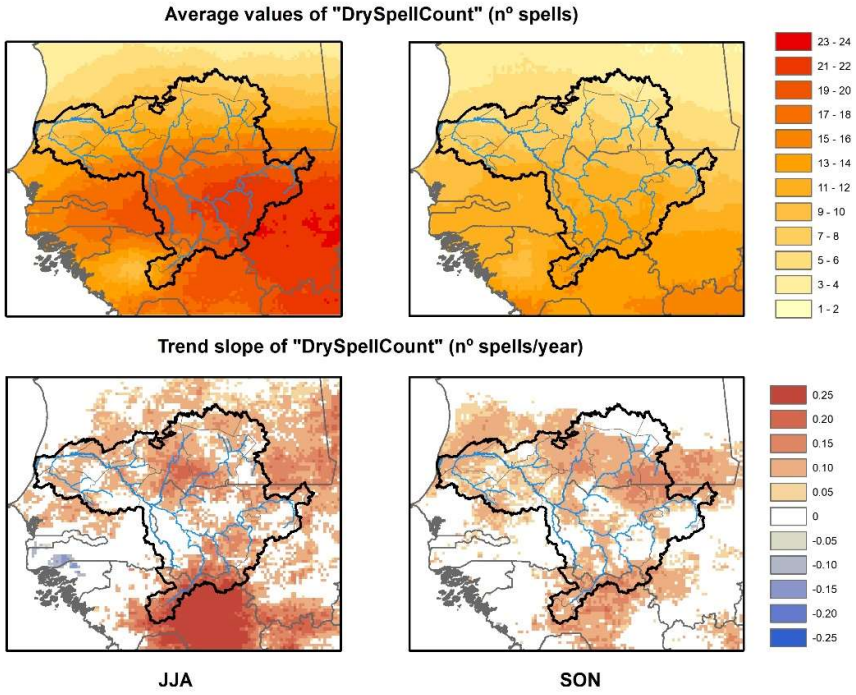

Figure 16: number of dry spells over Senegal River Basin from 1981 to 2016. Results are in form of average values (top) and trend slopes (down) for seasons JJA (left) and SON (right)

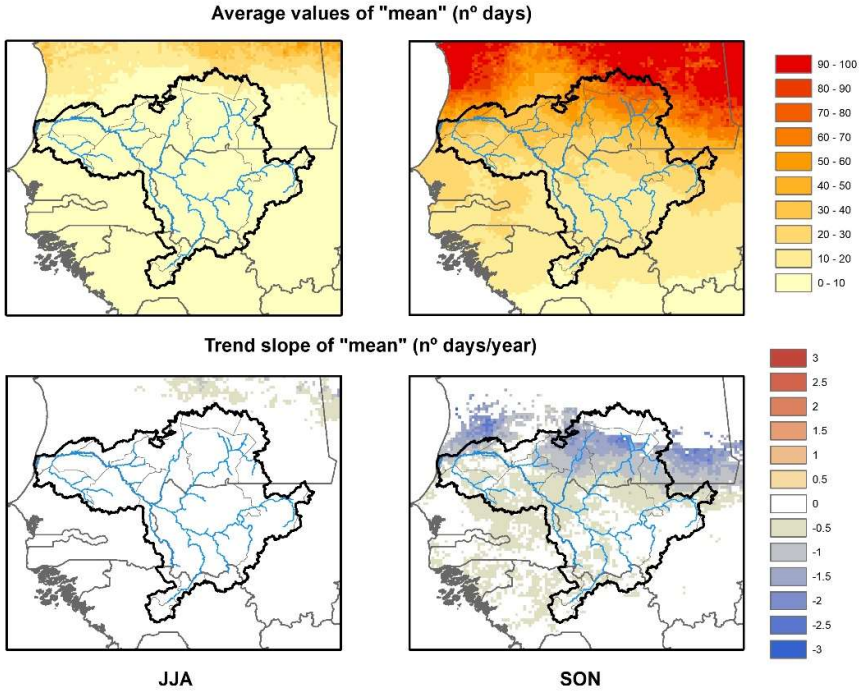

Figure 17: mean duration of dry spells over Senegal River Basin from 1981 to 2016. Results are in form of average values (top) and trend slopes (down) for seasons JJA (left) and SON (right)

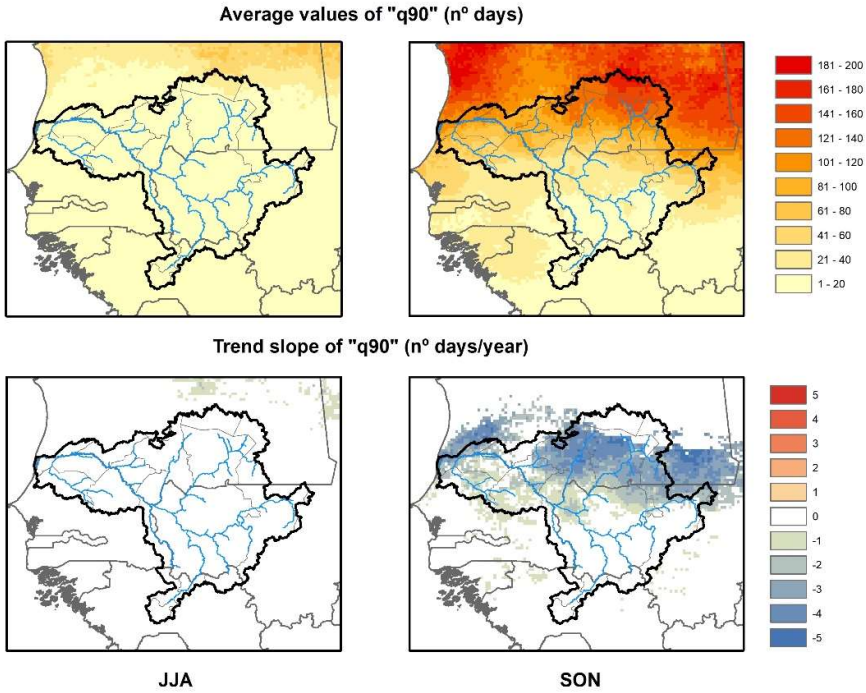

Figure 18: 90th percentiles of dry spells over Senegal River Basin from 1981 to 2016. Results are in form of average values (top) and trend slopes (down) for seasons JJA (left) and SON (right)

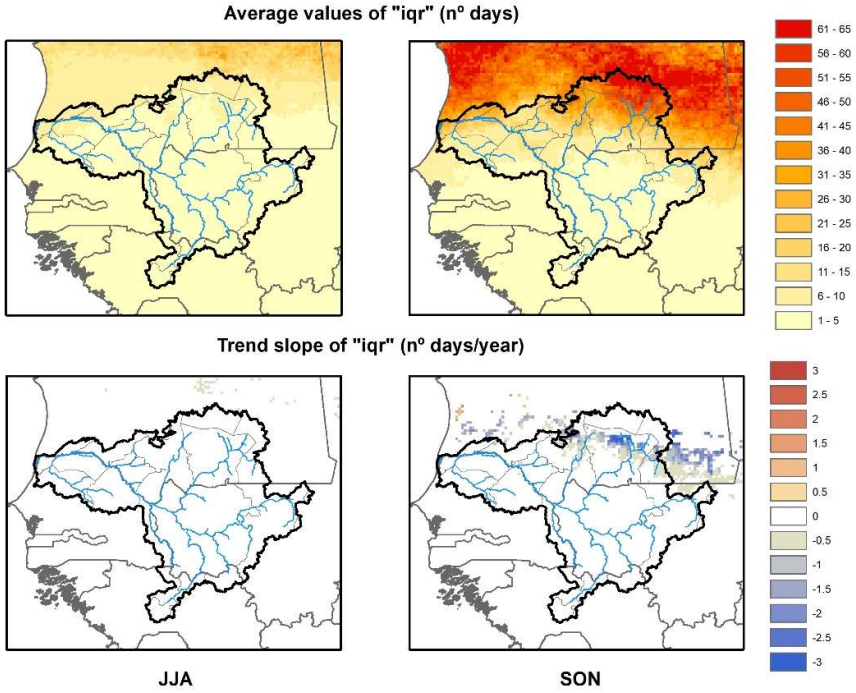

Figure 19: interquartile differences (between 75th and 25th percentiles) of dry spells over Senegal River Basin from 1981 to 2016. Results are in form of average values (top) and trend slopes (down) for seasons JJA (left) and SON (right)

The average results, evaluated as the first L-Moment, of the number of dry spells of short duration (3-9 days) related to the two seasons (*DrySpellCountLow*) respectively show a slightly higher frequency during JJA, reaching values of 8 in the central regions, while in SON they don't exceed a mean of 4 occurrences (Figure 15). As for their trends, slopes are mostly negligible, with localized peaks of 0.15 days/year in northern regions and on the western coast in JJA, and even less considerable values in SON.

As for the average number of dry spells (*DrySpellCount*), the occurrences generally increase while approaching to the south-eastern region of Koulikoro (Figure 16). A stronger incidence is encountered in the JJA period, with higher values measuring over 20 spells, while in SON they rarely exceed values of 15. Trend analysis shows a general growing behaviour over a good part of the basin area (up to 0.25 spells/year), with a particular emphasis on the southern end.

The average duration of dry spells (*mean*) is represented in Figure 17. From the images, it is evident that the longer dry spells occur in the northern region in the second half of rainy season (SON), reaching cases of almost 100 days in some points of the area; conversely, JJA is characterised by short spells seldom exceeding the duration of 10 days. In terms of trend slope, the only relevant variations are registered in months SON with general negative trend reaching peaks of -2 days/year in the northern region of Hodh el Gharbi.

The analysis of 90th percentile (*q90*) allows estimating the intensity of longest dry spells over the entire period. Output maps (Figure 18) show that extreme cases tend to verify in season SON over the northern regions, hitting average values of 200 days, whereas other one have cases rarely exceeding 30 days of length. Anyway, it has to be noticed that

almost all the areas affected by long spells are also interested by a generalised negative trend with tails of -5 days/year.

Lastly, outcomes of interquartile range (*iqr*) evaluation show the variability rate of the dry spell phenomenon within the whole basin area, as seen in Figure 19. JJA results return a limited gap between 25^{th} and 75^{th} percentiles (no more than 10 days) and no relevant trends. In the other period, differences are more pronounced especially in the north, reaching gap values over 60 days, but also in this case are affected by a negative trend (-3 days/year).

The overall impression provided by such results is that the first half of rainy season (JJA) is potentially affected by a considerable number of dry spells with average length (supposedly between 10 and 20 days) with a slightly increasing trend over the years. Conversely, SON period can be described with a larger statistical distribution with a more pronounced deviation and higher peaks, showing less occurrences yet with longer durations, especially in northern area, even if they register a negative trend over the entire period. However, given the presence of the desert in the north, characterized by a reduced precipitation rate, it can be expected to have extreme and unstable values in these areas. Results agree with the others previously obtained (Bichet et al., 2018), according to which, the West African Sahel shows an increasing number of dry spells, but their duration have a clear decreasing trend.

4 Global Surface Water Analysis

4.1 Improving Global Surface Water (GSW) usability in a computational resources-poor environment

GSW (Global Surface Water) is a key JRC data source (Pekel et al., 2016) for assessing surface water trends in space and time, as well as related impacts, e.g. on groundwater hydrology, flooding and the environment. Derived from LANDSAT images, the GSW has a spatial resolution of about 30 m and temporal monthly frequency, starting from early 1984. GSW is fully integrated within the distributed computing platform GEE (Google Earth Engine) and hence can be easily included in any quantitative analysis. The GSW reports information on the presence of water or land on a pixel-by-pixel basis, further to the unfortunate not-detected condition that often affects optical remote sensing, e.g. in presence of cloud coverage, sensor-related errors or lower image acquisition/exchange rates especially over Africa (Wulder et al., 2016, Busker et al., 2018).

Given its relevance, computation time can turn to be a major bottleneck in large scale applications, also when using GEE, despite its distributed and disconnected computing capabilities. Large African watersheds, as the Nile, Niger, Senegal, Congo and Zambezi, are currently the focus of major ongoing projects at JRC, as the ACEWATER2 (https://en.unesco.org/eu-partnership/science/acewater) and the WEFE-Senegal. Computation of overall statistics at basin scale, possibly disaggregated by sub-basins and/or administrative divisions can be done in GEE, but it may require advanced programming skills. Downloading and processing data locally is another option, which would however demand for storage capabilities and clustering computation facilities. A research centre can provide access to them, but this option is not open to most other users.

GEE is freely accessible for research purposes in academic and non-economic environments, but not for industrial/commercial applications, and most developing countries suffering for the digital divide would not even have access to a sufficiently stable internet connection to effectively make use of the platform.

Given the aforementioned framework, it was decided to investigate the opportunities deriving from image compression. Most of the above mentioned large scale applications aim at assessing evidence of major trends, addressing general issues as, for example, whether surface water bodies are shrinking or expanding, that would possibly lead to impacts on sensitive environments (as humid areas or groundwater) and being related to major evidences in climate trends. In these applications, the local details of pixel spatial arrangement have low relevance, if none at all. Hence, the GSW images can be resampled at a lower resolution, provided that the information on the area of each class (water, land, not detected) is preserved as from the original 30 m dataset (Figure 20).

Assuming that local spatial arrangement of pixels can be discarded as a minor information for large-scale applications, the GSW product can be simply resampled at the desired lower resolution. For each class, a new image is computed, reporting at each cell the overall number of pixels belonging to the class in the original image. This leads to a strong compression, reaching a 1/10000 ratio in case of a resampling over 100x100 pixels (3x3 km). Even taking account all the three classes (water, land, not detected), the overall reduction rate would be larger than 1/3,000.

An application for original GSW data resampling was originally developed in Python and R, and then migrated to C# for performance reasons, leading to more than one order of magnitude computational time improvement. As a further step, it will be implemented into E-Nexus as a dedicated tool.

A spatiotemporal database schema was designed to host the resampled GSW datasets, extending the original vector Hydro data model (Maidment, 2002) with explicit raster datasets support. The database was then implemented using state-of-the-art open source

spatiotemporal platform PostgreSQL (with PostGIS extension). Spatiotemporal analysis algorithms were then implemented in native spatially extended SQL, and later integrated in the above application.

Actually, the application masks out the majority of the implementation details. The system administrator is in charge of more challenging tasks, still kept very simple, as resampling new datasets, once available, and uploading the resampled datasets to the spatiotemporal database. On the other hand, the end user is simply expected to:

i. provide the geographical area(s) of interest

ii. select the variable(s) of interest

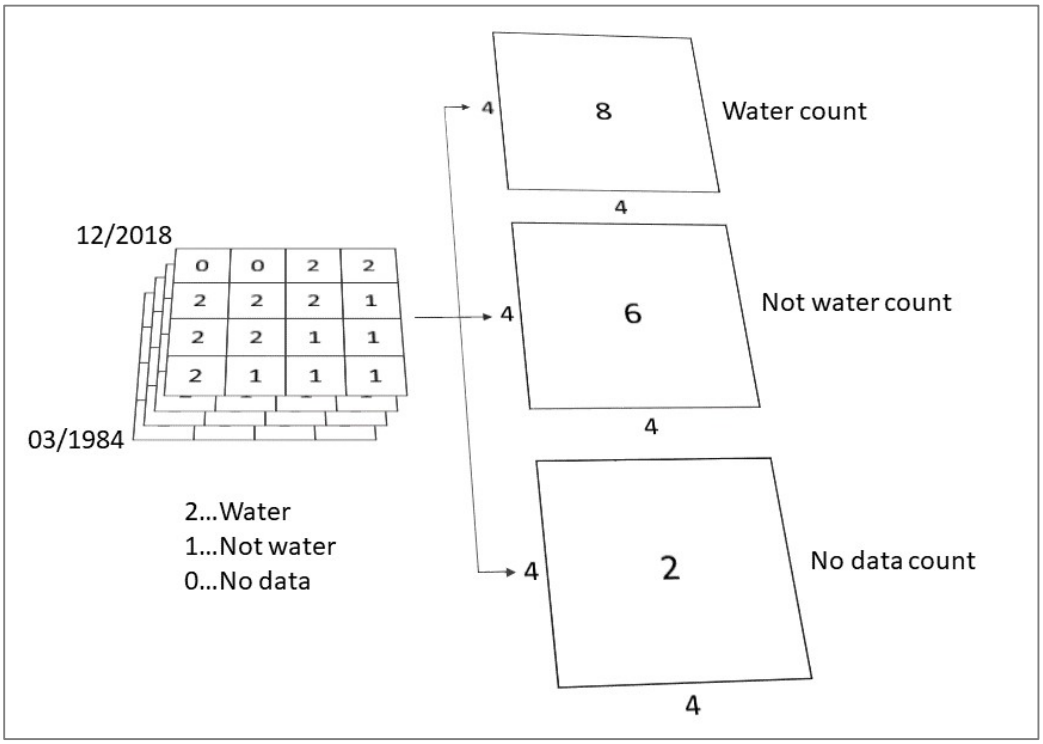

Figure 20: resampling approach of GSW monthly data

The application will access the database, compute and return the desired statistics over the entire available time series, making use of the computational facilities of the database platform. This solution will avoid data duplication deriving from exporting data outside of the database, as well as any further complexity due to external file formats. Most advanced users will also able to write their own spatiotemporal SQL queries to be run on the database, and, if desired, they will be able to link to the database from their own preferred analysis environments, as R or Python. It will also be possible to fully rely upon the internal database computation facilities for all the needed statistics.

As long as the database is managed as a central repository, different users can effectively access and share the same strategic data resource. Therefore, with the responsibility of database management on the shoulder of the database administrator, time loss and inherent risks deriving from duplication of data cleaning tasks will be minimized and centralized. In this way, end users will be able to focus on the analysis, much as is the case for the use of GEE.

Finally, it is worth to highlight that the same approach can be used for any classified image, as is the case for land use maps. The database has been designed to accommodate any

dataset, and spatial queries can address both different datasets and data types (vector and raster) without any further distinction.

4.2 Analysis of water surfaces in the Senegal River Basin using GSW data

Surface water analysis was carried out for the Senegal River Basin, its administrative regions and the four hydro-projects Manantali, Gouina, Felou and Diama, realized by the OMVS (Figure 21). The process involved the following two consistent GSW Water History datasets, referring to the period from March 1984 to December 2018 (version 1.1, 418 months):

i) Monthly Water History (MWH)
ii) Yearly Water Classification History (YC)

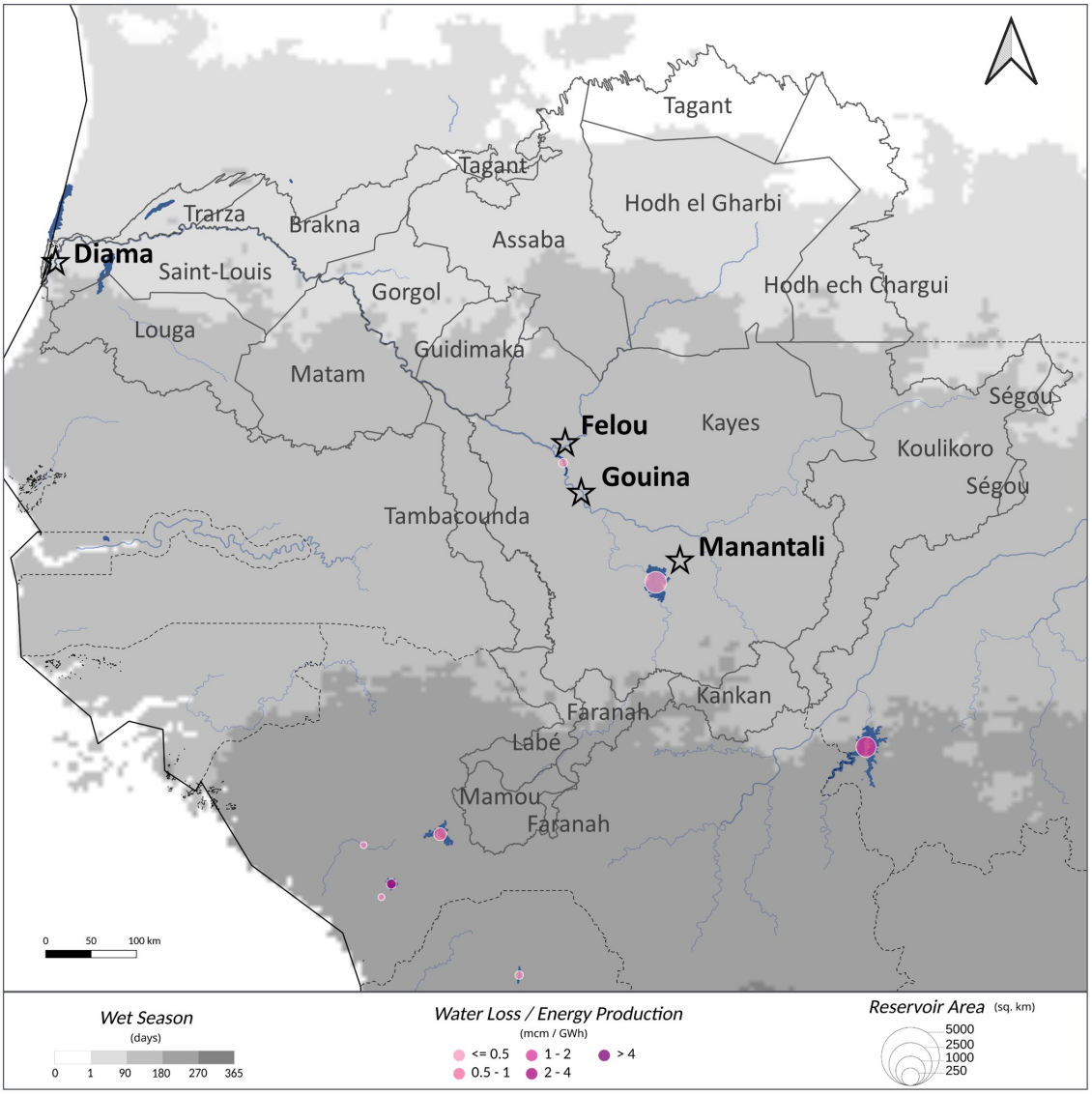

Figure 21: the Senegal River Basin, its administrative regions and the four hydro-projects Manantali, Gouina, Felou and Diama, realized by the OMVS. The ratio of (gross) water loss per energy production for year 2016 (circle colors) was analyzed for the two reservoirs of Manantali and Felou, used for hydropower production. The circle size indicates the reservoir areas [km²]. Wet season duration from Cordano (2018)

In addition, the GSW Mapping Layers (v1.1) were used to extract information about surface water occurrence, recurrence, seasonality, transition, change and maximum water extent (MWE) aggregated from the full time series. GSW data were extracted and processed using the Google Earth Engine platform (Gorelick et al., 2017), whereas water and no-data areas were extracted within the MWE. Monthly and yearly data from MWE with no-data ratios above 10% were not considered for analysis, keeping potential underestimation of water areas under 10%. The MWE represents the areas where water has been detected at least once during the full time series.

Water surfaces at River Basin level

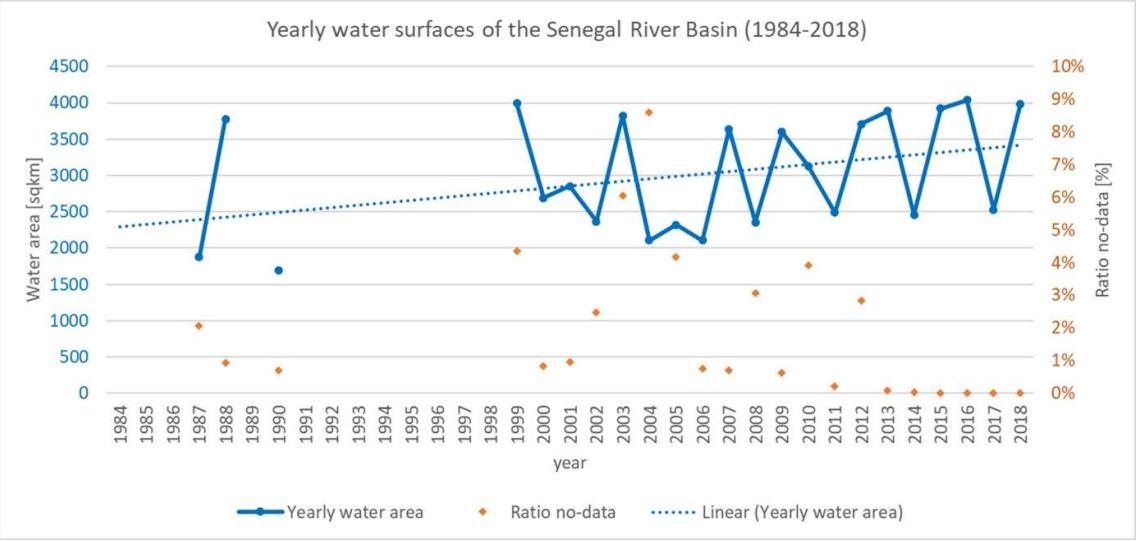

Figure 22: yearly water surfaces of the Senegal River Basin for the full time-series, derived from GSW Yearly Classification (YC). Years with no-data percentage above 10% were excluded

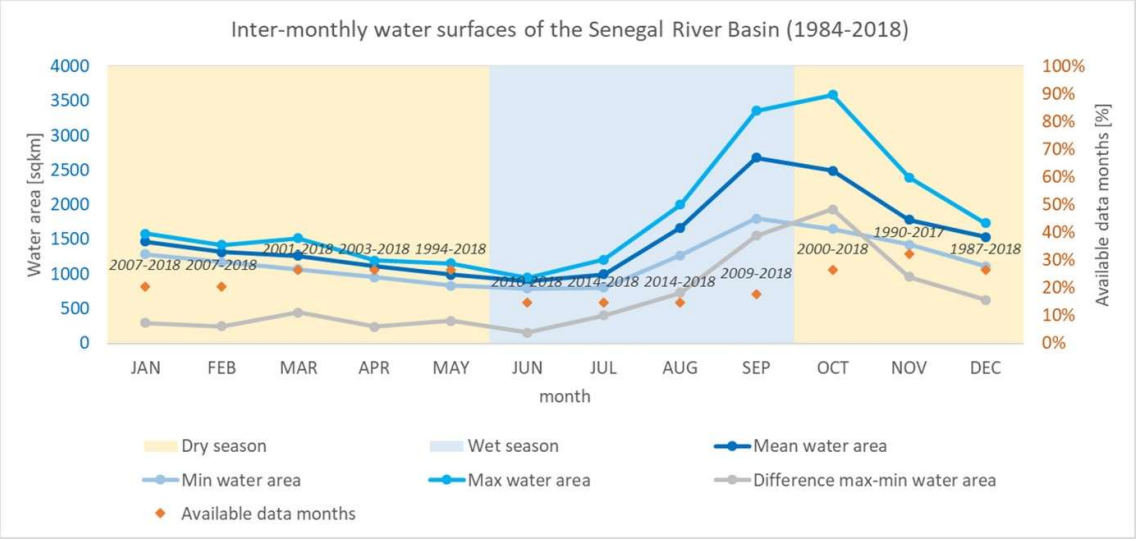

Figure 23: inter-monthly water surfaces of the Senegal River Basin for the full time-series, derived from GSW Monthly Water History (MWH). Months with no-data percentage above 10% were not considered for analysis, while orange dots represent the percentage of available data-months compared to all 418 months.

The yearly water surfaces in the Senegal River Basin show an increasing trend during the last 35 years (Figure 22). An oscillating behaviour can be observed, with one or two years

of smaller water surfaces (between 2000 and 2500 km^2) followed by one or two years of larger water surfaces (between 3500 and 4000 km^2). Data coverage of years with no-data ratios below 10% improves significantly from 1999 and 2013, which is mainly due to the launch of Landsat 7 (1999) and Landsat 8 (2013) (Wulder et al., 2016).

Smallest inter-monthly mean water surfaces in the Senegal River Basin are observed in June and July, the beginning of the wet season (Figure 23). Water surfaces remain in average below 1000 km^2 during this period. June is the month with the smallest difference between maximum and minimum water surfaces (158 km2), while October represents the biggest difference (1935 km^2). This implies a higher variability of water surfaces in the transition from wet to dry season. Relatively stable, but slightly decreasing water surfaces can be expected from January to June, in a long-term perspective. Highest mean of water areas are reached at the end of the wet season in September (2680 km^2).

Water surfaces at administrative region level

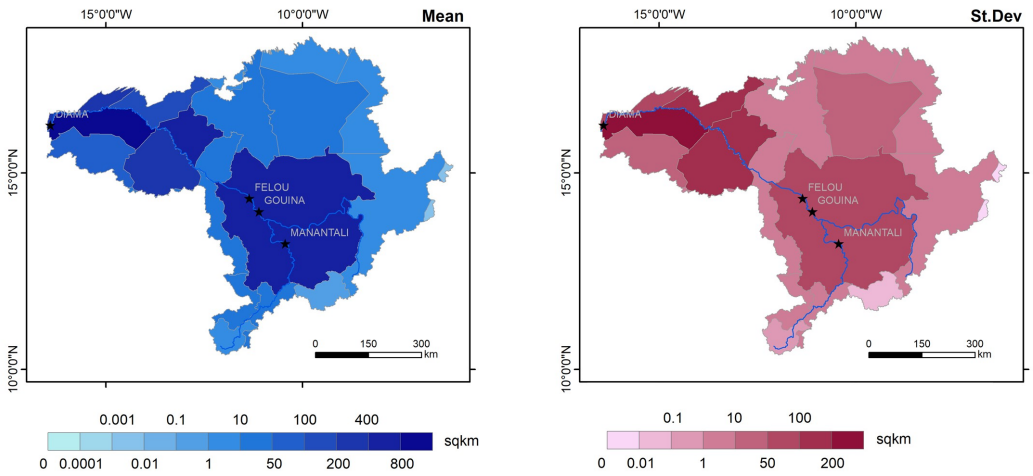

Figure 24: inter-annual water surfaces at administrative region level: mean and standard deviation

The distribution of inter-annual/monthly mean water surfaces at administrative region level is presented in the images from this paragraph. Figure 24 additionally highlights the standard deviation of annual water surfaces per region. The Saint Louis region shows the largest annual surface water mean (833 km^2) over the full time-series, followed by Kayes (628km^2) and Gorgol (527 km^2), mostly due to the presence of the major rivers such as Senégal, Bafing, Bakoy and Baoulé. The four hydro-projects (Figure 21) are located in these regions (Kayes and Saint-Louis). Almost no surface water (below 1 km^2) is detected throughout the year in the dry Northeast (Tagant, Hodh ech Chargui), East (Ségou) and South (Kankan) of the Basin. Inter-annual absolute change of water areas is higly significant in Saint Louis (st. dev.: 286 km^2), Matam (189 km^2) and Gorgol (132 km^2). Months featuring the largest mean water surfaces are September (736 km^2) in Saint Louis, November (600 km^2) in Kayes and October (528 km^2) in Gorgol (Figure 25)

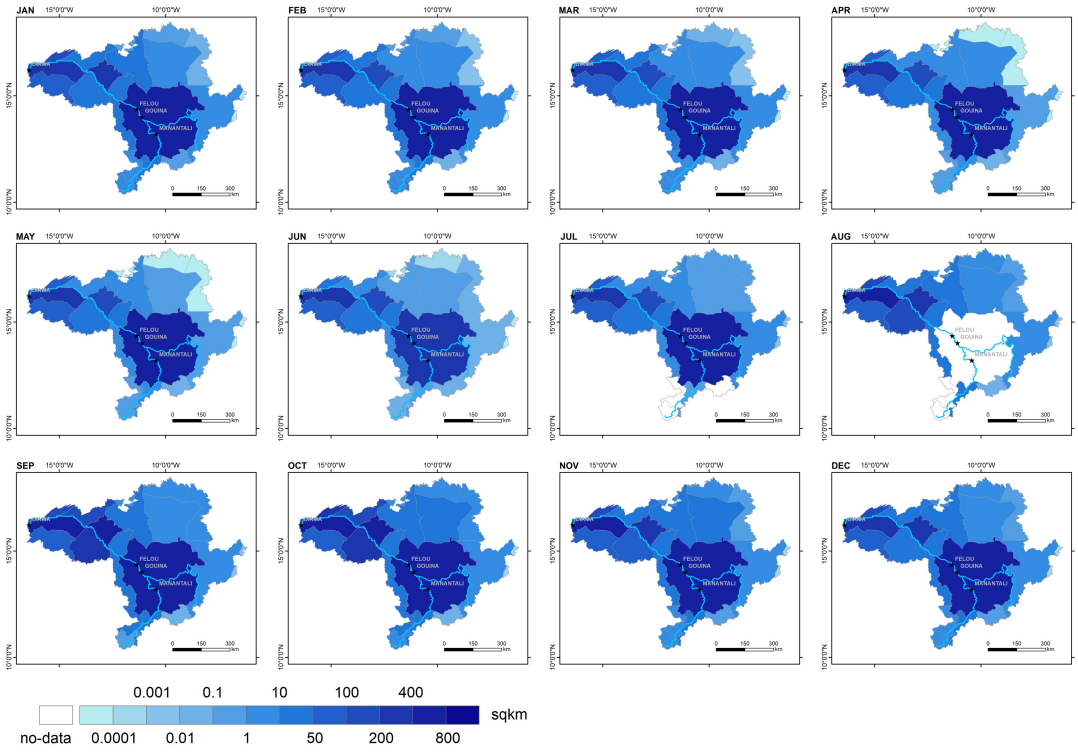

Figure 25: inter-monthly mean water surfaces at administrative region level, derived from GSW Monthly History (MWH). Months with no-data percentage above 10% were not considered for analysis

Water surfaces at hydro-project level

Four OMVS initiated hydro-projects have been realized in the Senegal River Basin for multiple purposes (Table 5, Figures 21 and 26). Manantali, Felou and Diama dams are in operation, whereas Gouina hydropower project is still under construction. The Diama project is the only dam which is not contributing to energy production, since it was mainly built to prevent salt water intrusion upstream the river in order to enable irrigated agriculture in the Senegal Plain. The Felou project is fully allocated to hydropower production, whereas water from Manantali reservoir is used for multiple purposes such as irrigation, flood control, energy production and navigation (OMVS, 2019; World Bank, 2017).

The frequency of water presence (occurrence) and the frequency of water return from year to year (recurrence) is very high at the Manantali reservoir and decreases only slightly along the reservoir edges. The number of months with water presence (seasonality) shows the same behaviour. The normalized change of water occurrence from 1984-1999 compared to 2000-2018 reveals generally stable water presence or a water gain in peripheral areas; areas of water loss are neglectable. This outcome indicates that the reservoir was already filled with water in the period between dam construction and dam commissioning (1988-2001), approved by the water areas detected in 1990 and 1994 (Figure 27) which has reached almost the reservoir extent as it was after dam commissioning.

	Manantali	Gouina*	Felou	Diama
Country	Mali	Mali	Mali	Senegal/Mauritania
Type	Reservoir	Run-of-River	Run-of-River	Run-of-River
River	Bafing	Senegal (Gouina Falls)	Senegal (Felou Falls)	Senegal
Construction Date	1982-1988	2016-today	1920s, 2009-2014	1981-1986
Commissioning/Opening Date	2001		1927, 2014	1986
Uses	I,FC,E,N	E	E	PSI, I, N
Installed Capacity	205	140	62.4	-

*Table 5: Characteristics of the four hydro-projects realized in the Senegal River Basin. I: Irrigation, FC: Flood Control, E: Energy Production, N: Navigation, PSI: Prevention of saltwater intrusion, *under construction*

The accumulation of the Bafing river took place from the end of dam construction in 1987/1988, causing a transition (classification of change between first and last year) towards new permanent (major reservoir areas) and new seasonal (reservoir edges) water areas forming the current Manantali reservoir. Felou and Gouina are run-of-the river hydroelectric plants causing only little water accumulation in the affected areas under analysis (Figure 26). In the case of Felou, some water gain is observed within a 5km distance from the plant, representing new permanent water surfaces. Remaining river areas show no change over time (seasonal oscillations are not considered).

Once operational, the impact of the Gouina plant on the river can be expected as similar compared to the one in Felou. However, the analysed river section of Felou shows more permanent water surfaces compared to Gouina: here, new permanent areas are observed very close to the Gouina plant followed by new seasonal water areas.

Diama is a transboundary gravity dam opened in 1986 crossing the border of Senegal and Mauritania. A dike extends the dam to the north in order to prevent saltwater intrusion: its intended effect becomes particularly evident with a massive change from water areas (salt water) to no water areas (-100%) within the analysed river section, while the freshwater surface of the Senegal River remains stable.

For the hydropower plants in Manantali and Felou, reservoirs annual water loss for year 2016 was determined and compared to the energy production of the hydropower plant (Table 6). The water loss is the product of reservoir area, evaporation rate and a ranking-based hydropower allocation factor for reservoirs used for multi-purposes (as the case for Manantali, Table 5). The energy production [GWh] is the product of capacity factor per country and the installed capacity [MW] of the hydropower plant, provided by PLATTS (2016). The capacity factor is a unit-less ratio of the actual versus the maximum possible electrical energy output. Yearly surface water information was obtained from GSW-YC. The evaporation rates from reservoirs were calculated using the LISVAP model (Alfieri et al., 2019; Burek, Van Der Knijff, and Ntegeka, 2013) and ERA5 data (Copernicus Climate Change Service, 2017).

In 2016, the Manantali reservoir had a surface area of 418km^2. Felou is a run-of-the-river hydropower plant located at the Felou Falls, covering a water area of 17 km^2. The water loss from Manantali reservoir amounts to 274 mcm (million cubic metres), while it is less than 30 mcm in Felou. The energy production of the Manantali plant amounts to 1230 GWh, a much higher value compared to the Felou plant (374 GWh). However, Felou performs better than Manantali when contrasting water loss with energy production (Figure 21).

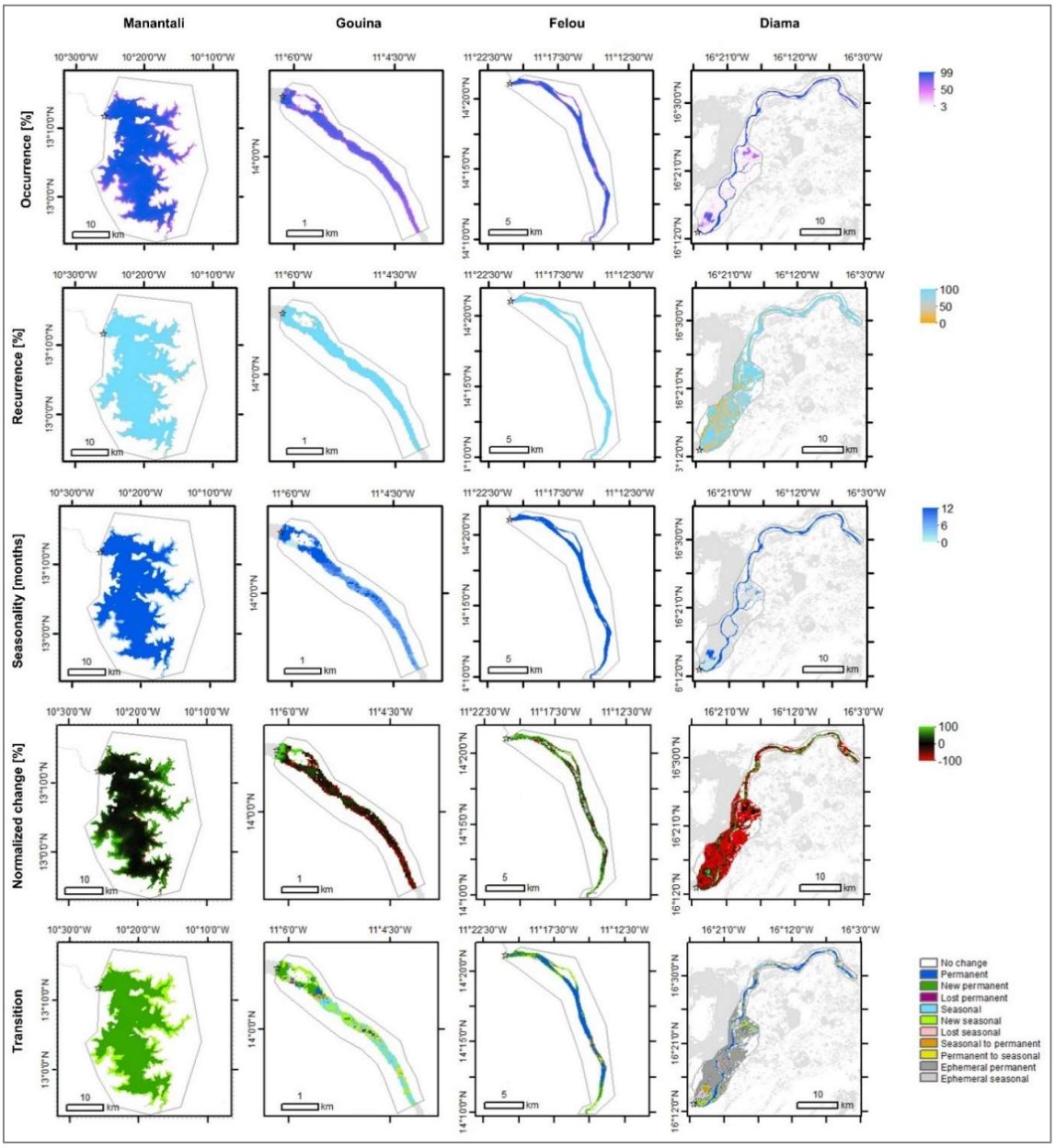

Figure 26: Occurrence, recurrence seasonality, normalized change and transition of water surfaces within the hydro-project affected regions (grey polygon). Light grey background areas represent the MWE of the full time-series (1984-2018). The black star indicates the dam/plant location.

Year 2016								
Name	IC	UAF	MWE	RA	EV	WL	EP	WL/EP
	MW	%	km2	km2	mm/yr	mcm	GWh	mcm/GWh
Manantali	205	0.33	453	418	1850	274	1230	0.22
Felou	62.4	1	17	16.52	1810	30	374	0.08

Table 6: Year 2016 water surfaces, gross water loss and energy production from Manantali and Felou reservoirs. IC: Installed Capacity, UAF: use allocation factor (0.33, meaning that hydropower is the third ranked use in this reservoir), RA: reservoir area, EV: evaporation, WL: water loss, EP: energy production, WL/EP: ratio water Loss vs energy Production (see Figure 21)

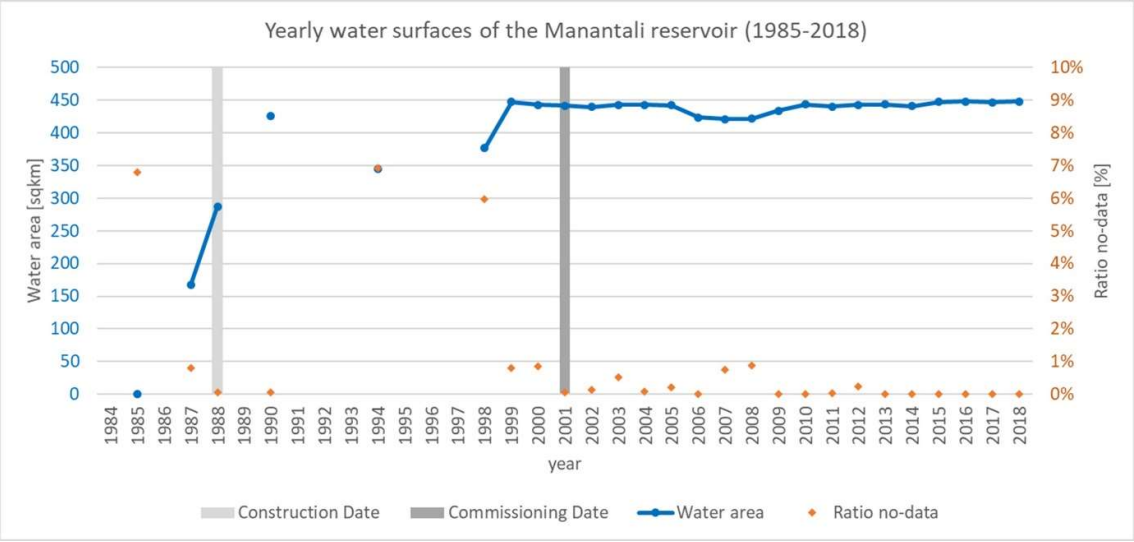

Figure 27: Yearly water surfaces of the Manantali reservoir before and after dam commissioning, for the full time-series, derived from GSW Yearly Classification (YC). Years with no-data percentage above 10% were excluded

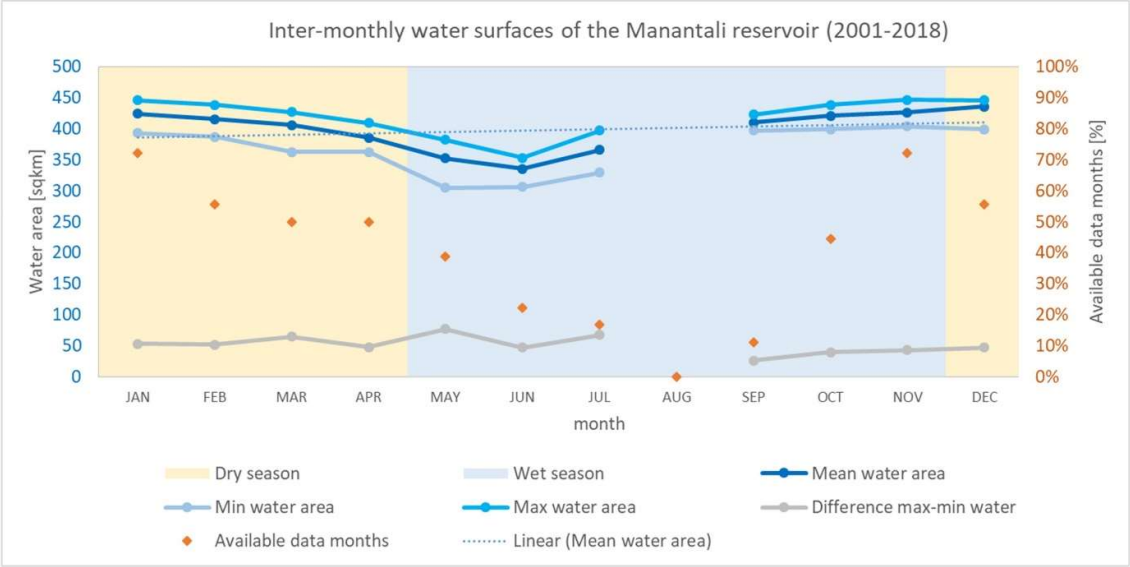

Figure 28: inter-monthly water surfaces of the Manantali reservoir after dam commissioning (2001-2018), derived from GSW Monthly History (MWH). Months with no-data percentage above 10% were not considered for analysis

The Manantali dam reservoir shows relatively stable annual reservoir surfaces of almost 450 km^2 since the commissioning of the dam in year 2001 (Figure 27). Only between 2006 and 2009, the water extent decreased to 410 km^2. Since it is a regulated reservoir, the decrease could have been caused by climate, by dam reservoir management or overexploitation. The inter-monthly means of water surfaces (Figure 28) reflect a similar but smoother trend as for the entire Senegal River Basin (Figure 23).

5 E-Nexus interface with eStation datasets

The E-Nexus is also able to interface via SFTP protocol to the remote data managers in order to have access to a multiple choice of datasets and use them as possible inputs for its climate variability process. So far, the interface has been configured to collect data gathered by the eStation, a platform mainly conceived for real-time meteorological purposes, and able to retrieve and process data both from EUMETcast and internet databases, providing a strong enhancement for already existing stations spreaded over African continent (Clerici et al., 2013).

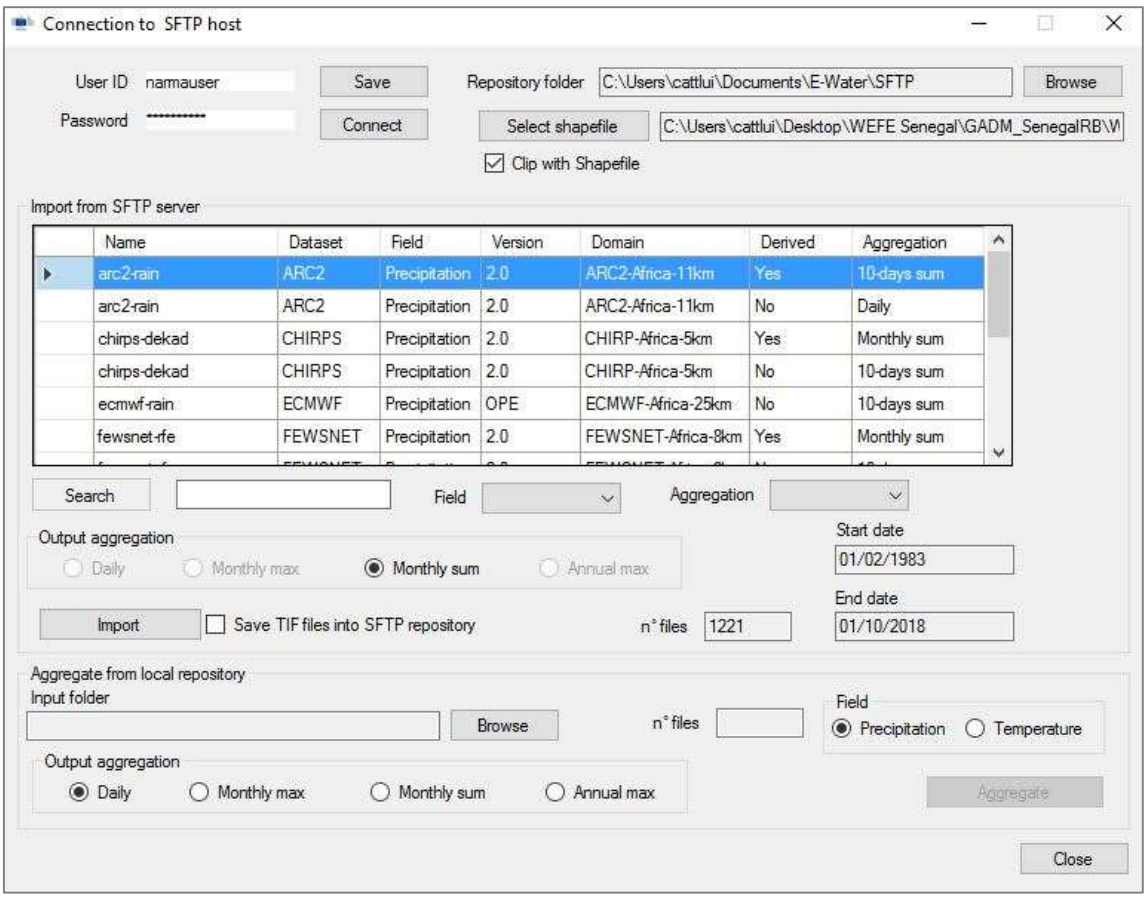

Figure 29: SFTP graphic interface from E-Nexus tool

Rather than simply connect to database and download files like any conventional FTP client, E-Nexus features a dedicated interdace able to let authorised user to directly access interested datasets in a few steps (see Figure 29). The interface automatically filters database files in order to quickly conduct user focusing exclusively on suitable data as for E-Nexus application: through the menu it is possible to easily visualise all available data series on a table providing detailed info about their source, version, field and domain, other than reporting about updated databases. Other than that, files are processed after download, and rearranged into one single NetCDF file, perfectly compatible for processes of the Climate module (Excess/Deficit, Heat Waves, etc.), even changing time scale and performing spatial filtering if needed (Cattaneo et Al., 2018).

Currently available adatasets are shown below on Table 7.

Name	Info
ARC-2	Daily precipitations from 1983 over Africa with 0.1º resolution (Novella et al., 2013)
CHIRPS	Daily to monthly precipitations from 1981 on quasi-global scale with 0.05º resolution (Funk et al., 2015)
ECMWF	Decadal global precipitations from 2008 with 0.25º resolution (site: https://www.ecmwf.int/)
FEWSNET	Decadal and monthly precipitations from 2001 over Africa with 8-km resolution (USGS, 2018)
TAMSAT	Decadal and monthly precipitations from 1983 over Africa with 0.375º resolution (Maidment et al., 2017)
LSASAF	Daily and decadal temperatures from 2015 over Africa with 1-km resolution (Trigo et al., 2011).
MODIS	Daily temperatures from 2002 over Africa with 4-km resolution (NASA, 2015)

Table 7: list of datasets provided by SFTP interface

For compatibility issues, only gridded datasets of temperature and precipitation series are available (the ones needed fro climate variability), but future improvements could also allow to provide other kind of inputs, introducing new variabiles and the possibility to access to station observations.

6 Conclusions and future steps

As the 2nd year of the WEFE Senegal project is reaching the end, this document gives an overall report of the current status of the E-Nexus tool as experimental version of a Decision Support System for Environmental Monitoring, and its results achieved in the analysis of environmental trends and anomalies at the river basin level.

Climate variability assessment shown on previous pages has been able to display a limited number of localized anomalies and relevant trends within the boundaries of Senegal River Basin. By the way, it is possible to improve performance and reliability by integrating obtained results with supplementary indices with a lesser dependency on climate aspects (e.g. land use). For instance, it can be said that values provided by dry spell analysis can also be compared with crop data (e.g. definition and guidelines for the sowing and growing periods of the different types of crop, harvesting data from crop modelling data), for a better comprehension of the relationship involving dry spells with agriculture and water/dam management. Even if dry spell variation results to be significantly low to be obtained by statistical analysis of gridded precipitation data, climate variability effects have a noticeable weight on rain-dependent and flood recession agricultural activities of the Senegal River Basin area.

It is worth to point that the module is currently updating specific tools for hydrology and agriculture modelling (SWAT and EPIC) other than performing a setup process on local data collection serving as input (refinement and calibration/validation, required for models), with first results expected for oncoming year. In addition, the development of Optimization menu – another tool provided by E-Nexus more focused on the resource management (water, crops) - requires multiple feedback and contribution from local stakeholders other than suitable input data. In fact, both parts have a considerable importance on many factors like the design of economic module, the identification of constraints to be included, and the identification of priorities and interconnection between components. Also, the development of E-Nexus in the frame of WEFE project may also involve the implementation of a new section regarding the analysis of energy production (through water dams and other sources) and supply management.

Another goal to be considered is to extend the E-Nexus data compatibility to local observations provided by on situ stations, thus providing additional information that helps the module to achieve a better reliability and consistency of produced outcomes.

Finally, the connection interface described in the last paragraph is currently set to a single SFTP site (the one serving eStation), but it could be easily exploited for a wider range of hosts. This would allow users to connect to multiple remote file managers and get data supply able to fit bigger demands and be more suitable for studies on specific areas within the basin, each featuring its size, position and environmental conditions.

References

Alfieri, L., V. Lorini, F. Hirpa, S. Harrigan, E. Zsoter, C. Prudhomme, and P. Salamon. 2019. A Global Streamflow Reanalysis for 1980-2018. Journal of Hydrology in review.

Agnew, C.T., 2000. Using the SPI to Identify Drought. Drought Netw. News 1.

Beck, H.E., E.F. Wood, M. Pan, C.K. Fisher, D.G. Miralles, A.I. van Dijk, T.R. McVicar, and R.F. Adler, 2019: MSWEP V2 Global 3-Hourly 0.1° Precipitation: Methodology and Quantitative Assessment. Bull. Amer. Meteor. Soc., 100, 473–500, https://doi.org/10.1175/BAMS-D-17-0138.1

Beck, H. E., van Dijk, A. I. J. M., Levizzani, V., Schellekens, J., Miralles, D. G., Martens, B., and de Roo, A.: MSWEP: 3-hourly 0.25° global gridded precipitation (1979–2015) by merging gauge, satellite, and reanalysis data, Hydrol. Earth Syst. Sci., 21, 589–615, https://doi.org/10.5194/hess-21-589-2017, 2017.

Bichet, A. and Diedhiou A. 2018. "West African Sahel Has Become Wetter During the Last 30 Years, but Dry Spells Are Shorter and More Frequent." *Climate Research* 75 (2): 155–62. doi:10.3354/cr01515.

Burek, Peter Andreas, Johan Van Der Knijff, and Victor Nyakatura Ntegeka. 2013. LISVAP Evaporation Pre-Processor for the LISFLOOD Water Balance and Flood Simulation Model.

Busker, T., de Roo, A., Gelati, E., Schwatke, C., Adamovic, M., Bisselink, B., Cottam, A. (2018). A global lake and reservoir volume analysis using a surface water dataset and satellite altimetry. Hydrology and Earth System Sciences Discussions, (January), 1–32. https://doi.org/10.5194/hess-2018-21

Cattaneo, L.; Carmona, C.; Pastori, M, e-NEXUS Remote connection menu. A practical interface to eStation database, European Commission, Ispra, 2018 Publication, JRC115137.

Cattaneo L., Pastori M., Cordano E., Carmona C., E-Nexus Senegal - A DSS for the analysis of WEFE Nexus in the Senegal river basin - Climate Variability , European Commission, Ispra, 2018, JRC115134.

Ceccherini, G., Russo, S., Ameztoy, I., Marchese, A.F., Carmona-Moreno, C., 2017. Heat waves in Africa 1981-2015, observations and reanalysis. Nat. Hazards Earth Syst. Sci. 17, 115–125. https://doi.org/10.5194/nhess-17-115-2017

Chaudhary, Shushobhit, C.T. Dhanya, and R. Vinnarasi. 2017. Dry and Wet Spell Variability during Monsoon in Gauge-Based Gridded Daily Precipitation Datasets over India. Journal of Hydrology 546: 204–18. doi: https://doi.org/10.1016/j.jhydrol.2017.01.023.

Clerici, M., Combal, B., Pekel, J.F., Dubois, G., van't Klooster, J., Skøien, J.O., Bartholomé, E., 2013. The eStation, an Earth Observation processing service in support to ecological monitoring. Ecol. Inform. 18, 162–170. https://doi.org/10.1016/J.ECOINF.2013.08.004

Cohn, A.S., Newton, P., Gil, J.D.B., Kuhl, L., Samberg, L., Ricciardi, V., Manly, J.R., Northrop, S., 2017. Smallholder Agriculture and Climate Change, Annual Review of Environment and Resources. https://doi.org/10.1146/annurev-environ-102016-060946

Copernicus Climate Change Service 2017. ERA5: Fifth generation of ECMWF atmospheric reanalysis of the Global Climate. Copernicus Climate Change Service Climate Data Store (CDS). Retrieved August 12, 2019 (https://cds.climate.copernicus.eu/cdsapp#!/home).

Cordano, Emanuele. 2015. RGENERATEPREC: Tools to Generate Daily-Precipitation Time Series. http://CRAN.R-project.org/package=RGENERATEPREC.

Cordano, E. (2018). Estimation of wet season duration in a year. Retrieved August 7, 2019, from https://aquaknow.jrc.ec.europa.eu/acewater2-jrc/dataset/estimation-wet-season-duration-year

FAO, 2016. The State of Food and Agriculture: Climate Change, Agriculture and Food Security. https://doi.org/ISBN: 978-92-5-107671-2 I

Froidurot, Stéphanie, and Arona Diedhiou. 2017. "Characteristics of Wet and Dry Spells in the West African Monsoon System." Atmospheric Science Letters 18 (3): 125–31. doi:10.1002/asl.734.

Funk, C., Peterson, P., Landsfeld, M., Pedreros, D., Verdin, J., Shukla, S., Husak, G., Rowland, J., Harrison, L., Hoell, A. and Michaelsen, J. (2015) The climate hazards infrared precipitation with stations — a new environmental record for monitoring extremes. Scientific Data volume 2, Article number: 150066 doi:10.1038/sdata.2015.66

Gorelick, N., Hancher, M., Dixon, M., Ilyushchenko, S., Thau, D., and Moore, R. (2017). Google Earth Engine: Planetary-scale geospatial analysis for everyone. Remote Sensing Environment

Gornall, Jemma, Richard Betts, Eleanor Burke, Robin Clark, Joanne Camp, Kate Willett, and Andrew Wiltshire. 2010. "Implications of Climate Change for Agricultural Productivity in the Early Twenty-First Century." Philosophical Transactions of the Royal Society B: Biological Sciences 365 (1554): 2973–89. doi:10.1098/rstb.2010.0158.

Guttman, N.B. (1999), ACCEPTING THE STANDARDIZED PRECIPITATION INDEX: A CALCULATION ALGORITHM1. JAWRA Journal of the American Water Resources Association, 35: 311-322. doi:10.1111/j.1752-1688.1999.tb03592.x

Hersbach, H., P. de Rosnay, B. Bell, D. Schepers, A. Simmons, C. Soci, S. Abdalla, M. Alonso Balmaseda, G. Balsamo, P. Bechtold, P. Berrisford, J. Bidlot, E. de Boisséson, M. Bonavita, P. Browne, R. Buizza, P. Dahlgren, D. Dee, R. Dragani, M. Diamantakis, J. Flemming, R. Forbes, A. Geer, T. Haiden, E. Hólm, L. Haimberger, R. Hogan, A. Horányi, M. Janisková, P. Laloyaux, P. Lopez, J. Muñoz-Sabater, C. Peubey, R. Radu, D. Richardson, J.-N. Thépaut, F. Vitart, X. Yang, E. Zsótér & H. Zuo, 2018: Operational global reanalysis: progress, future directions and synergies with NWP, ECMWF ERA Report Series 27.

Hosking, J.R.M., 2017. L-Moments. R package, version 2.6. URL: https://CRAN.R-project.org/package=lmom.

Lesk, C., Rowhani, P., Ramankutty, N., 2016. Influence of extreme weather disasters on global crop production. Nature 529, 84–87. https://doi.org/10.1038/nature16467

Lipper, L., Thornton, P., Campbell, B.M., Baedeker, T., Braimoh, A., Bwalya, M., Caron, P., Cattaneo, A., Garrity, D., Henry, K., Hottle, R., Jackson, L., Jarvis, A., Kossam, F., Mann, W., McCarthy, N., Meybeck, A., Neufeldt, H., Remington, T., Sen, P.T., Sessa, R., Shula, R., Tibu, A., Torquebiau, E.F., 2014. Climate-smart agriculture for food security. Nat. Clim. Chang. 4, 1068–1072. https://doi.org/10.1038/nclimate2437

Maidment D.R., 2002. Arc Hydro: GIS for Water Resources. ESRI Press, Redlands, CA, USA

Maidment, R.I., Grimes, D., Black, E., Tarnavsky, E., Young, M., Greatrex, H., Allan, R.P., Stein, T., Nkonde, E., Senkunda, S., Alcántara, E.M.U., 2017. A new, long-term daily satellite-based rainfall dataset for operational monitoring in Africa. Sci. Data 4, 170063. https://doi.org/10.1038/sdata.2017.63

Masupha, Teboho Elisa, Mokhele Edmond Moeletsi, and Mitsuru Tsubo. 2016."Dry Spells Assessment with Reference to the Maize Crop in the Luvuvhu River Catchment of South Africa. Physics and Chemistry of the Earth, Parts A/B/C 92: 99–111. doi:https://doi.org/10.1016/j.pce.2015.10.014.

Mckee, T.B., Doesken, N.J., Kleist, J., 1993. The Relationship of Drought Frequency and Duration Times Scales, in: American Meteorological Society. 8th Conference on Applied Climatology 17-22 Janvier, Anaheim. pp. 179–184.

NASA, 2015. MODIS Characterization Support Team (MCST)/MODIS Adaptive Processing System (MODAPS). https://doi.org/http://dx.doi.org/10.5067/MODIS/MOD01.006

Novella, N. S., Thiaw, W. M. 2013. African rainfall climatology version 2 for Famine Early Warning Systems. J. Appl. Meteor. Climatol., 52, 588–606, https://doi.org/10.1175/JAMC-D-11-0238.1.

OMVS, 2019. Domaines d'intervention. Retrieved from http://www.omvs.org/content/domaines-dintervention

Pekel, Jean François, Andrew Cottam, Noel Gorelick, and Alan S. Belward. 2016. High-Resolution Mapping of Global Surface Water and Its Long-Term Changes. Nature 540(7633):418–22.

PLATTS 2016. World Electric Power Plants Database. Retrieved August 18, 2019 (https://www.platts.com/products/world-electric-power-plants-database).

Ratan, R., and V. Venugopal. 2013. Wet and Dry Spell Characteristics of Global Tropical Rainfall. Water Resources Research 49 (6): 3830–41. doi:10.1002/wrcr.20275.

Russo, S., Dosio, A., Graversen, R. G., Sillmann, J., Carrao, H., Dunbar, M. B., Singleton, A., Montagna, P., Barbola, P., and Vogt, J. V. (2014), Magnitude of extreme heat waves in present climate and their projection in a warming world, *J. Geophys. Res. Atmos.*, 119, 12,500– 12,512, doi: 10.1002/2014JD022098.

Russo, S., Sillmann, J., Fischer, E.M., 2015. Top ten European heatwaves since 1950 and their occurrence in the coming decades. Environ. Res. Lett. 10, 124003. https://doi.org/10.1088/1748-9326/10/12/124003

Trigo, I.F., Dacamara, C.C., Viterbo, P., Roujean, J.-L., Olesen, F., Barroso, C., Camachode- Coca, F., Carrer, D., Freitas, S.C., García-Haro, J., Geiger, B., Gellens- Meulenberghs, F., Ghilain, N., Meliá, J., Pessanha, L., Siljamo, N., Arboleda, A., 2011. The Satellite Application Facility for Land Surface Analysis. Int. J. Remote Sens. 32, 2725–2744. https://doi.org/10.1080/01431161003743199

Udias, A., Pastori, M., Dondeynaz, C., Carmona Moreno, C., Ali, A., Cattaneo, L., Cano, J., 2018. A decision support tool to enhance agricultural growth in the Mékrou river basin (West Africa). Comput. Electron. Agric. 154, 467–481. https://doi.org/10.1016/J.COMPAG.2018.09.037

USGS, 2018. FEWS Home. Early Warning and Environmental Monitoring Program [WWW Document]. URL https://earlywarning.usgs.gov/fews (accessed 12.12.18).

Van Keulen, H., Breman, H., 1990. Agricultural development in the West African Sahelian region: a cure against land hunger? Agric. Ecosyst. Environ. 32, 177–197.

World Bank. 2017. Senegal - OMVS Transmission Expansion Project (English). Washington, D.C.: World Bank Group. http://documents.worldbank.org/curated/en/923211494813685983/Senegal-OMVS-Transmission-Expansion-Project

Wulder, M. A., White, J. C., Loveland, T. R., Woodcock, C. E., Belward, A. S., Cohen, W. B., Roy, D. P. (2016). The global Landsat archive : Status, consolidation, and direction. Remote Sensing of Environment, 185, 271–283.

Zougmoré, R., Partey, S., Ouédraogo, M., Omitoyin, B., Thomas, T., Ayantunde, A., Ericksen, P., Said, M., Jalloh, A., 2016. Toward climate-smart agriculture in West Africa: a review of climate change impacts, adaptation strategies and policy developments for the livestock, fishery and crop production sectors. Agric. Food Secur. 5, 26. https://doi.org/10.1186/s40066-016-0075-3

List of figures

List of tables

GETTING IN TOUCH WITH THE EU

In person

All over the European Union there are hundreds of Europe Direct information centres. You can find the address of the centre nearest you at: https://europa.eu/european-union/contact_en

On the phone or by email

Europe Direct is a service that answers your questions about the European Union. You can contact this service:

- by freephone: 00 800 6 7 8 9 10 11 (certain operators may charge for these calls),

- at the following standard number: +32 22999696, or

- by electronic mail via: https://europa.eu/european-union/contact_en

FINDING INFORMATION ABOUT THE EU

Online

Information about the European Union in all the official languages of the EU is available on the Europa website at: https://europa.eu/european-union/index_en

EU publications
You can download or order free and priced EU publications from EU Bookshop at: https://publications.europa.eu/en/publications. Multiple copies of free publications may be obtained by contacting Europe Direct or your local information centre (see https://europa.eu/european-union/contact_en).

The European Commission's science and knowledge service

Joint Research Centre

JRC Mission

As the science and knowledge service of the European Commission, the Joint Research Centre's mission is to support EU policies with independent evidence throughout the whole policy cycle.

EU Science Hub

ec.europa.eu/jrc

@EU_ScienceHub

EU Science Hub - Joint Research Centre

Joint Research Centre

EU Science Hub

Publications Office